On chemical reaction planar fronts in an elastic–viscoelastic mechanical framework

Svetlana Petrenko, Alexander B Freidin, Eric Charkaluk

Svetlana Petrenko · Alexander B. Freidin · Eric Charkaluk

On chemical reaction planar fronts in an elastic–viscoelastic mechanical framework

Abstract A stress-affected chemical reaction front propagation is considered using the concept of a chemical affinity tensor. A reaction between an elastic solid constituent and a diffusing constituent, localized at the reaction front, is considered. As a result of the reaction, the elastic constituent transforms into viscoelastic one. The reaction is accompanied by volume expansion that in turn may result in stresses at the reaction front, which affect the front velocity through the normal component of the chemical affinity tensor. Considering a plane strain problem with a planar chemical reaction front propagation under uniaxial deformation, we focus on the studies of the reaction front kinetics in dependence on external strains and material parameters with the use of the notion of the equilibrium concentration. Then, stress relaxation behind the propagating reaction front is modeled. A standard linear solid model is used for the reaction product, and its particular cases are also considered. Analytical solutions are obtained which allow to study in explicit form the strain influence and material parameters on the front retardation or acceleration and stress relaxation.

Keywords Mechanochemistry · Chemical affinity tensor · Reaction front kinetics · Stress relaxation · Standard linear solid model

1 Introduction

The influence of stress–strain state on chemical reactions has been widely considered since the 70s of the last century. The oxidation of silicon in nanowires, e.g., [2], or in MEMS, e.g., [36], reactions in ceramic composites with inclusions, e.g., [37], lithiation of silicon in Li-ion batteries, e.g., [32], can be mentioned among the examples that demonstrate the importance of establishing interconnections between stress-affected chemical reactions and the stress–strain state at the reaction front (see also [20,33,46] and the references in [14]).

The above-mentioned and many other reactions can be described using a two-phase reaction model in which the reaction is localized at the sharp interface—a reaction front, and the diffusing reactant is transported to the reaction front through the transformed solid material. One of the first and most simple models that described such reactions was the model proposed by Deal and Grove based on a planar reaction front [6]. This model

gave a general scenario of the problem statement but did not consider stress effects (see also [11,14] where this model is described in the context of introducing a chemical affinity tensor). However, chemical reactions can be accompanied by volumetric expansion that produces internal stresses, which in turn may affect the chemical reaction (see, e.g., [7,27,37]). An extension of the Deal–Grove model was proposed by considering a stress-dependent diffusion coefficient and a reaction rate constant, e.g., [22,28,43]. Other alternatives to take into account the influence of stresses on the diffusion and the reaction are to introduce additional terms in the expression of the diffusion flux, e.g., [25,26], or to consider the influence through a scalar chemical potential [1,29,30].

In fact, stresses may affect the reaction front propagation via the influence on the diffusivity, e.g., [22], or additional stress-gradient terms in the diffusion flux, e.g., [25]. This case can be referred as diffusion-controlled reactions. But the front propagation may be affected by stresses via the direct influence on the reaction rate, see, e.g., [4]. This corresponds to the case of the reaction front propagation controlled rather by the reaction rate than by the diffusion, and lithiation is an example of such a reaction (see, e.g., [21,47]).

In the present paper, we focus on the second case. Modeling of the reaction front kinetics is based on the chemical affinity tensor. The expression of the chemical affinity tensor was derived initially in [8] for the case of a chemical reaction between diffusing and nonlinear elastic constituents as a tensor defining a thermodynamic force conjugate to the front velocity in the expression of the energy dissipation due to the front propagation, similar to the derivation made in [24] for a propagating phase interface in a nonlinear elastic solid. Then, it was derived from fundamental balance laws and the entropy inequality written down for an open system with a chemical reaction between diffusing and solid constituents of arbitrary rheology in the case of finite strains (see [9,10,15] and a review [14]). It was shown that the normal component of this tensor acts as a thermodynamic force conjugated to the reaction rate in the expression of the energy dissipation due to the front propagation, and a kinetic equation in the form of the dependence of the reaction rate on the normal component of the affinity tensor was formulated.

In a quasi-static case, the chemical affinity tensor is represented by the linear combination of the chemical potential tensors, which are the Eshelby energy–momentum tensors divided by the reference mass densities. This combination is the same as the combination of scalar chemical potentials which defines the classical chemical affinity (see, e.g., [41]), and the notion of the chemical affinity arises to pioneering works by Gibbs [16] and de Donder [5]. Therefore, the consideration based on the affinity tensor is consistent with the approach of classical physical chemistry where reaction rate is determined by a scalar chemical affinity. Since the reaction front velocity is defined by the reaction rate, in the framework of the mechanics of configurational forces [19,23,31], the affinity tensor determines the configurational force driving the reaction front.

Note that the tensorial nature of the chemical affinity in the case of solid constituents follows from the consideration of a chemical reaction on the oriented area element of the reaction front (see a more detailed discussion in [14]), as well as the tensorial nature of the chemical potential followed from the fact that a phase equilibrium took place not just in a point but at the oriented area elements of the phase interface passing through the point (see, e.g., [18] and reference therein).

The approach based on the chemical affinity tensor has been applied to the statement and solution of a number of boundary value problems with propagating reaction fronts for the case of linear elastic solid constituents [11,12,15,44]. Then, the theory has been used to describe numerically two-phase lithiation of Si particles used in Li-ion batteries, where the constituent materials undergoing finite elasto-viscoplastic deformations were considered [39,40].

In the present paper, we come back to the case of small strains and, at first, study in detail the influence of elastic moduli of the solid constituents on the reaction front behavior in dependence on external strains. Then, we develop a model for analytical studies of stress relaxation behind the reaction front which relevance is motivated by the fact that reaction products often exhibit viscous rather than elastic behavior, e.g., [22]. The difference of molar volumes of initial and transformed materials is a source of volume expansion due to a chemical reaction. Kinematic compatibility, i.e., displacement continuity at the reaction front, restricts the expansion and produces stresses which could be huge in the case of a pure elastic behavior. Viscoelastic assumptions allow the strain to be partly accommodated by the viscous deformation, and the stresses can relax (see, e.g., [3,7,27]). In addition, since the total thickness of the transformed layer is observed in experiments with planar reaction fronts, even simple models may be useful for the estimation of the impacts of the transformation and viscous strains on the thickening during the front propagation.

The paper is organized as follows. A short summary of the concept of the chemical affinity tensor is given in Sect. 2, along with the formulation of a general quasi-static coupled problem involving mechanics, diffusion and chemistry. This is followed in Sect. 3 by the formulation and solution of the problem for a

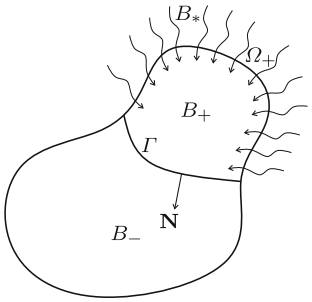

Fig. 1 Chemical reaction between solid and diffusive constituents; Γ is the reaction front

planar reaction front propagation in a plate made initially of a linear elastic material that becomes viscoelastic after the reaction. A standard linear solid model is taken for the reaction product. The kinetic equation for the propagating reaction front and detailed studies of the influence of elastic moduli and an energy parameter on the front propagation and blocking are presented. Then, the derivations and solutions of the equations for the stress relaxation and inelastic strains description behind the propagating front are given and discussed. Conclusions are presented in Sect. 4.

2 General framework

In this section, a brief summary of the concept of chemical affinity tensor, that is used in the present paper, is given. More detailed explanations can be found in [9,10,14,15].

2.1 Chemical affinity tensor: kinetic equation

A chemical reaction between solid and diffusing constituents of the following type is considered:

$$n_- B_- + n_* B_* \longrightarrow n_+ B_+,$$

where B_-, B_* and B_+ are the chemical formulae of initial solid, diffusing and transformed solid constituents, respectively; n_-, n_* and n_+ are the stoichiometric coefficients. The reaction is localized at the reaction front Γ that divides the solid constituents B_- and B_+, and it is sustained by the diffusion of B_* through the reaction product B_+ (see Fig. 1).

Note that chemical reactions may be accompanied by large transformation strains, and the general theory based on the chemical affinity tensor was developed for finite strains. But further a small strain approach is used that allows to obtain analytical solutions and to demonstrate the features of problem setting and the influence of parameters on the behavior of the reaction front in an analytically controlled way.

Other simplifications relate to diffusion and are motivated by focusing on the front propagation controlled by the reaction rate and the direct influence of stresses on the reaction rate. The simplest Fick's diffusion law with stress-independent diffusivity coefficient is accepted. The transformed material B_+ is considered as a solid skeleton for the diffusing constituent B_*, i.e., we neglect the deformations which could be produced in the transformed material by the diffusing constituent. We also neglect the influence of the pressure produced by the diffusing constituent on total stresses, implying that the hydrostatic part of the stresses produced by the transformation strains is much greater. Note that the diffusion is affected by stresses even in this case, but not through the constitutive equation of the diffusion but through the boundary conditions at the propagating stress-affected reaction front. The thermal effects of the chemical reaction are also neglected, and the temperature T is assumed to be a given parameter.

To describe the chemical reaction front kinetics, we use an approach based on the concept of chemical affinity tensor. As it was mentioned in Introduction, the normal component of the chemical affinity tensor appears in the expression of the energy dissipation due to the reaction front propagation. It was shown that the dissipation Dis per unit area of the propagating reaction front takes the forms

$$\mathrm{Dis} = \frac{\rho_-}{n_- M_-} A_{\mathrm{NN}} V_{\mathrm{N}} = A_{\mathrm{NN}} \omega(\mathbf{N}), \tag{2.1}$$

where ρ_- is the mass density of the initial material B_-, V_N is the normal component of the reaction front velocity, $\omega(\mathbf{N})$ is the reaction rate at the reaction front area element with normal $\mathbf{N}$, and $A_{\mathrm{NN}} = \mathbf{N}\cdot\mathbf{A}\cdot\mathbf{N}$ is the normal component of the tensor $\mathbf{A}$, called the chemical affinity tensor. In a quasi-static case

$$\mathbf{A} = n_- M_- \mathbf{M}_- + n_* M_* \mu_* \mathbf{I} - n_+ M_+ \mathbf{M}_+, \tag{2.2}$$

where $\mathbf{M}_-$ and $\mathbf{M}_+$ are the chemical potential tensors which are equal to the Eshelby energy–momentum tensors, divided by the reference mass densities of solid constituents B_- and B_+, μ_* is the chemical potential of the diffusing constituent, $\mathbf{I}$ is the second-rank identity tensor, and $M_{\pm,*}$ are the molar masses of $B_{\pm,*}$, respectively. It is used in (2.1) that the normal component V_N of the front velocity is related to the reaction rate as

$$V_\mathrm{N} = \frac{n_- M_-}{\rho_-}\omega(\mathbf{N}). \tag{2.3}$$

Note the similarity between the expressions (2.1) of the dissipation with the affinity tensor (2.2) and the classical expressions of the dissipation $\mathrm{Dis} = A\omega$ with the scalar chemical affinity $A = -\sum n_k M_k \mu_k$, where ω is the reaction rate in a point, μ_k are the scalar chemical potentials of the constituents, and the stoichiometric coefficients $n_k (k = 1, 2...)$ are substituted into the sum with the sign "+" if the k-th constituent is produced in the reaction and with the sign "−" if the constituent is consumed by the reaction [41].

One can see in (2.1) that A_{NN} is a thermodynamic force conjugate to the reaction rate at the oriented area element, and, therefore, a kinetic equation can be formulated in the form of the dependence of the reaction rate $\omega(\mathbf{N})$ on A_{NN}. Then, from Eq. (2.3) it follows that A_{NN} also determines the reaction front velocity. Since the velocity V_N determines changing the configuration of the body, it is natural, in the spirit of the mechanics of configurational forces [19,23,31], to treat the multiplier conjugate to V_N in the dissipation formula as the configurational force. Thus, the chemical affinity tensor defines the configurational force driving the reaction front, similarly to how the jump of the Eshelby energy–momentum tensor defines the configurational force driving a phase interface in the case of stress-induced phase transformations (see, e.g., [45]).

The substitution of the normal component A_{NN} of the chemical affinity tensor into a known relationship between the reaction rate and the scalar chemical affinity, valid for the wide range of chemical reactions (see, e.g., [17]), instead of a scalar chemical affinity gives the following formula for the reaction rate $\omega(\mathbf{N})$ at the reaction front area element with normal $\mathbf{N}$ [9]:

$$\omega(\mathbf{N}) = k_* c\left(1 - \exp\left(-\frac{A_{\mathrm{NN}}}{RT}\right)\right), \tag{2.4}$$

where k_* is the reaction rate constant, R is the universal gas constant, and c is the molar concentration of the diffusing constituent per unit volume.

Then, from (2.3) and (2.4) it follows that the dependence of the normal component of the reaction front velocity on the normal component of the affinity tensor can be taken as [9,10,15]:

$$V_\mathrm{N} = \frac{n_- M_-}{\rho_-} k_* c\left(1 - \exp\left(-\frac{A_{\mathrm{NN}}}{RT}\right)\right). \tag{2.5}$$

Further we will use kinetic equations (2.4) and (2.5) rewritten in terms of a current and so-called equilibrium concentrations of the diffusing constituent [9,15]. The equilibrium concentration c_{eq} corresponds to chemical equilibrium such that

$$A_{\mathrm{NN}}(c = c_{\mathrm{eq}}) = 0. \tag{2.6}$$

By the skeleton approach, the tensors $\mathbf{M}_\pm$ in the expression (2.2) do not depend on the concentration. Then, the mechanical part of A_{NN} is related to c_{eq} as

$$n_- M_- \mathbf{N}\cdot\mathbf{M}_-\cdot\mathbf{N} - n_+ M_+ \mathbf{N}\cdot\mathbf{M}_+\cdot\mathbf{N} = -n_* M_* \mu_*(c_{\mathrm{eq}}), \tag{2.7}$$

and the normal component of the affinity tensor can be expressed via the difference of the chemical potentials of the diffusing constituent calculated at the current concentration $c(\Gamma)$ and the equilibrium concentration c_{eq} found for stresses and strains at the front:

$$A_{\mathrm{NN}} = n_* M_* \left(\mu_*(c(\Gamma)) - \mu_*(c_{\mathrm{eq}})\right). \tag{2.8}$$

To avoid misunderstanding, note that the equilibrium concentration is defined by Eq. (2.6) irrespective of the diffusion problem.

The chemical potential of the diffusing constituent is specified further as

$$M_*\mu_* = f_* + RT\ln\frac{c}{c_*}, \tag{2.9}$$

where f_* and c_* are the reference chemical energy and concentration of the diffusing constituent, respectively. Then, in the case of small strains the normal component of the chemical affinity tensor takes the form [10,11,15]:

$$A_{\mathrm{NN}} = \frac{n_-M_-}{\rho_-}(\gamma - \chi) + n_*RT\ln\frac{c}{c_*} \tag{2.10}$$

where

$$\chi = w_+ - w_- - \boldsymbol{\sigma}_\pm : [\![\boldsymbol{\varepsilon}]\!] \tag{2.11}$$

characterizes the input of stresses and strains, $w_\pm$ are the strain energies of the solid constituents per unit volume, $[\![\boldsymbol{\varepsilon}]\!] = \boldsymbol{\varepsilon}_+ - \boldsymbol{\varepsilon}_-$ is the jump of the strain tensor across the reaction front, $\boldsymbol{\varepsilon}_\pm$ are the strains of the materials $B_\pm$,

$$\gamma = f_0^- - f_0^+ + \frac{\rho_-}{n_-M_-}n_*f_* \tag{2.12}$$

is the temperature-dependent energy parameter equal to the combination of the chemical energies $f_0^\mp$ of the solid constituents $B_\mp$ (Helmholtz free energies of solids in stress-free states) and the reference energy f_* of the diffusing constituent, and γ is taken further as a parameter of the model.

Note that since the traction $\mathbf{t} = \boldsymbol{\sigma}\cdot\mathbf{N}$ is continuous across the reaction front, from the displacement and traction continuity it follows that the stresses $\boldsymbol{\sigma}_\pm$ on any side of the front can be substituted into $\boldsymbol{\sigma}_\pm : [\![\boldsymbol{\varepsilon}]\!]$ in (2.11). Indeed, since, due to the continuity of displacements, the jump of strain tensor is represented in the form

$$[\![\boldsymbol{\varepsilon}]\!] = \frac{1}{2}(\mathbf{a}\otimes\mathbf{N} + \mathbf{N}\otimes\mathbf{a}), \tag{2.13}$$

where $\mathbf{a}$ is the jump amplitude, the following equalities are valid:

$$\boldsymbol{\sigma}_- : [\![\boldsymbol{\varepsilon}]\!] = \mathbf{a}\cdot\boldsymbol{\sigma}_-\cdot\mathbf{N} = \mathbf{a}\cdot\boldsymbol{\sigma}_+\cdot\mathbf{N} = \boldsymbol{\sigma}_+ : [\![\boldsymbol{\varepsilon}]\!].$$

During further analysis, the stoichiometric coefficients are normalized by n_*:

$$n_- \to n_-/n_*, \quad n_+ \to n_+/n_*, \quad n_* \to 1.$$

Then, by Eqs. (2.4), (2.5), (2.8) and (2.9), the reaction rate and the reaction front velocity are expressed directly through the current concentration of the diffusing constituent and the equilibrium concentration corresponding to the stresses and strains at the front (see, e.g., [11]):

$$\omega(\mathbf{N}) = k_*\left(c(\Gamma) - c_{\mathrm{eq}}\right), \quad V_{\mathrm{N}} = \frac{n_-M_-}{\rho_-}k_*\left(c(\Gamma) - c_{\mathrm{eq}}\right), \tag{2.14}$$

where, by (2.6) and (2.10), c_{eq} is determined by the formula

$$\frac{c_{\mathrm{eq}}}{c_*} = \exp\left\{-\frac{n_-M_-}{\rho_-}\frac{(\gamma-\chi)}{RT}\right\}. \tag{2.15}$$

In such a representation, stresses and strains affect the reaction rate via the equilibrium concentration, and one can see that the front may propagate only if $c(\Gamma) > c_{\mathrm{eq}}$.

2.2 Problem statement

To find the reaction front velocity, one has to know stresses and strains at the front, to calculate c_{eq} and to solve the diffusion problem. To find stresses in a quasi-static case, in the absence of body forces, one has to solve the equilibrium equation

$$\nabla \cdot \boldsymbol{\sigma} = 0, \tag{2.16}$$

where $\boldsymbol{\sigma}$ is the Cauchy stress tensor. The equation (2.16) is to be solved within domains υ_- and υ_+, which are occupied by materials B_- and B_+, respectively, with boundary conditions at the outer surface of the body (forces or displacements are prescribed), interface conditions at the reaction front (continuity of the displacement $\mathbf{u}$ and traction) and with constitutive equations of solid constituents.

To find the concentration c, we assume that the diffusion flux $\mathbf{j}_*$ is given by Fick's law

$$\mathbf{j}_* = -D\nabla c,$$

where D is the diffusion coefficient of the reactant B_* through B_+. We assume that D is a constant. We neglect the initial stage of the diffusion prior to the start of the reaction at the outer boundary of the body. Considering that the front propagation is controlled by the reaction rate rather than by the diffusion rate, we assume that the diffusion process is happening on much faster timescale than the chemical reaction and is fast enough to consider a steady-state diffusion. Then, the diffusion is described by the Laplace equation

$$\Delta c = 0 \tag{2.17}$$

with the boundary conditions

$$D\frac{\partial c}{\partial N}\bigg|_{\Omega_+} - \alpha\,(c_* - c(\Omega)) = 0, \quad D\frac{\partial c}{\partial N}\bigg|_{\Gamma} + \omega(\mathbf{N}) = 0, \tag{2.18}$$

where Ω_+ is the part of the outer surface of the body through which the diffusion flux is supplied, it is the external boundary of the transformed material (Fig. 1), c_* is the solubility of B_* in the material B_+, and α is the mass transfer coefficient. Without loss of generality, one may take c_* also as the reference volume density in Eqs. (2.9) and (2.10).

The first boundary condition states that the diffusion flux through the outer boundary of the body becomes zero if the solubility c_* is reached. The second condition means that all the diffusing reactant is fully consumed at the reaction front and with the use of Eq. (2.14) can be rewritten as

$$D\frac{\partial c}{\partial N}\bigg|_{\Gamma} + k_*\left(c(\Gamma) - c_{\text{eq}}\right) = 0. \tag{2.19}$$

Eventually, we come to the coupled problem for a solid with propagating interface which velocity depends on the concentration of a diffusing matter and mechanical stresses at the interface, while the concentration and stresses depend on the position of the interface. All the equations are summarized in the following set of equations (see the box below). Note that this set of equations is valid for any constitutive models of solid constituents.

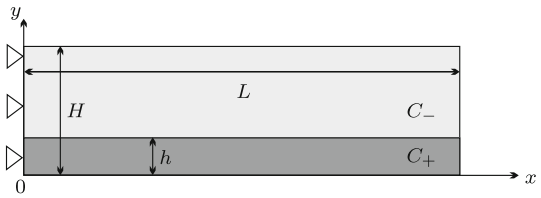

Fig. 2 Plane strain problem for a plate with a planar reaction front

Equilibrium equation:

$$\nabla \cdot \boldsymbol{\sigma} = 0, \qquad [\![\boldsymbol{\sigma}]\!]|_\Gamma \cdot \mathbf{N} = 0, \ [\![\mathbf{u}]\!]|_\Gamma = 0 \quad + \quad \text{B.C.}$$

Constitutive equations of solid constituents.
Equilibrium concentration: $c_{\text{eq}}: \ A_{\text{NN}}|_{c=c_{\text{eq}}} = 0,$

$$\frac{c_{\text{eq}}}{c_*} = \exp\left\{-\frac{n_- M_-}{\rho_-}\frac{(\gamma - \chi)}{RT}\right\}, \quad \chi = w_+ - w_- - \boldsymbol{\sigma}_\pm : [\![\boldsymbol{\varepsilon}]\!].$$

Diffusion problem: $\Delta c = 0,$

$$D\frac{\partial c}{\partial N}\bigg|_{\Omega_+} - \alpha\,(c_* - c(\Omega_+)) = 0,$$
$$D\frac{\partial c}{\partial N}\bigg|_{\Gamma} + k_*\left(c(\Gamma) - c_{\text{eq}}\right) = 0.$$

Chemical reaction front kinetics:

$$V_{\text{N}} = \frac{n_- M_-}{\rho_-} k_*\left(c(\Gamma) - c_{\text{eq}}\right) = 0.$$

3 A chemical reaction front propagation in the case of a linear viscoelastic reaction product

3.1 Reaction front kinetics

To demonstrate the influence of the viscosity on the reaction front kinetics, we consider in this section the simple plane strain problem for a chemical reaction in a plate of thickness H and length $L >> H$ with a planar reaction front (see Fig. 2). The reaction starts at the outer surface $y = 0$ of an initially elastic plate. The planar reaction front propagates in the y-direction, and the reaction front position is given by $y = h$. The lower $y = 0$ and upper $y = H$ faces of the plate are traction free. Displacement u_0 at the edges $x = \pm L$ prescribes the strain $\varepsilon_0 = u_0/L$ in x-direction. Therefore, the strains have to satisfy the following conditions:

$$\varepsilon_z = \varepsilon_{xz} = \varepsilon_{yz} = 0, \quad \varepsilon_x = \varepsilon_0.$$

The diffusion problem is reduced to the diffusion equation

$$\frac{\mathrm{d}^2 c}{\mathrm{d}y^2} = 0, \quad y \in [0, h] \tag{3.1}$$

with boundary conditions

$$D\left.\frac{\mathrm{d}c}{\mathrm{d}y}\right|_{y=0} = \alpha(c(0) - c_*), \quad D\left.\frac{\mathrm{d}c}{\mathrm{d}y}\right|_{y=h} = -k_*(c(h) - c_{\text{eq}}). \tag{3.2}$$

From the solution of the diffusion problem (3.1), (3.2), it follows that the concentration of the diffusing constituent B_* at the reaction front is equal to

$$c(h) = \frac{c_* + k_* \left(\dfrac{h}{D} + \dfrac{1}{\alpha} \right) c_{\text{eq}}}{1 + k_* \left(\dfrac{h}{D} + \dfrac{1}{\alpha} \right)}. \tag{3.3}$$

Then, by Eq. (2.14), the reaction front velocity can be calculated as

$$V = \frac{n_- M_-}{\rho_-} \frac{c_* - c_{\text{eq}}}{\dfrac{1}{k_*} + \dfrac{1}{\alpha} + \dfrac{h}{D}}, \tag{3.4}$$

where the equilibrium concentration c_{eq}, defined by Eq. (2.15), depends on stresses and strains at the reaction front.

Formula (3.4) can be rewritten as

$$\dot{\xi} = \frac{n_- M_-}{\rho_-} \frac{c_* - c_{\text{eq}}}{T_{\text{ch}} + T_{\text{D}} \xi},$$

where $\xi = \dfrac{h}{H}$, the dot denotes the time derivative, and the characteristic times of diffusion and chemical reaction, T_{D} and T_{ch}, are defined by formulae

$$T_{\text{D}} = \frac{H^2}{D}, \quad T_{\text{ch}} = H \left(\frac{1}{k_*} + \frac{1}{\alpha} \right). \tag{3.5}$$

In the stress problem, the equilibrium equations and the boundary conditions are satisfied in the Saint–Venant sense if one takes in the plate

$$\sigma_y = 0, \qquad \sigma_{xy} = 0. \tag{3.6}$$

From continuity of the displacement, it follows that at the reaction front

$$[\![\varepsilon_x]\!] = 0.$$

Then, from Eq. (3.6) and plane strains conditions it follows that $\boldsymbol{\sigma}_- : [\![\boldsymbol{\varepsilon}]\!] = 0$ in the expressions (2.10), (2.11) for the normal component of the chemical affinity tensor.

We assume that the initial material "$-$" is isotropic linear elastic. Then, due to the plane strains conditions, by Hooke's law, in the elastic layer $y \in [h, H]$ the stresses

$$\sigma_x^- = \frac{4\mu_- (3k_- + \mu_-)}{3k_- + 4\mu_-} \varepsilon_0, \quad \sigma_z^- = \frac{2\mu_- (3k_- - 2\mu_-)}{3k_- + 4\mu_-} \varepsilon_0,$$
$$\sigma_{zx} = \sigma_{zy} = 0, \tag{3.7}$$

where k_- and μ_- are the bulk and shear modules of the material B_-. Then, the strain energy density of the material B_- is

$$w_- = \frac{2\mu_- (3k_- + \mu_-)}{3k_- + 4\mu_-} \varepsilon_0^2. \tag{3.8}$$

For the inelastic material "$+$," we assume that volumetric strains are elastic, and inelastic behaviors are represented by rheological models formulated as relationships between deviatoric parts of stress and strain tensors. Then, we use the following decompositions

$$\boldsymbol{\sigma} = \sigma \mathbf{I} + \mathbf{s}, \qquad \boldsymbol{\varepsilon} = \frac{\vartheta}{3} \mathbf{I} + \mathbf{e}, \tag{3.9}$$

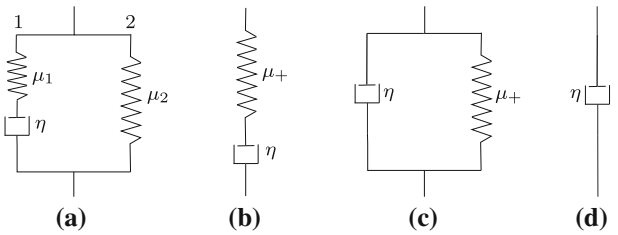

Fig. 3 Rheological viscoelastic models: **a** standard linear solid model, **b** Maxwell model, **c** Kelvin–Voigt model, **d** linear viscous model

where $\sigma = \frac{1}{3}\mathrm{tr}\,\boldsymbol{\sigma}$ and $\vartheta = \mathrm{tr}\,\boldsymbol{\varepsilon}$ denote the hydrostatic parts of the stress tensor and volume strain, and $\mathbf{s}$ and $\mathbf{e}$ are the deviatoric stress and strain, respectively.

We assume that the transformation strain is spherical: $\boldsymbol{\varepsilon}^{\mathrm{tr}} = (\vartheta^{\mathrm{tr}}/3)\mathbf{I}$. Then, the hydrostatic parts of the stress tensor and volume strain are related in constituent "+" as

$$\sigma^+ = k_+(\vartheta^+ - \vartheta^{\mathrm{tr}}). \tag{3.10}$$

To study how the viscosity and the specified choice of the viscoelastic rheology of the transformed material affect the stress redistribution due to the chemical reaction, we take at first the standard linear solid model (SLSM) (Fig. 3a) that was also referred as the Poynting–Thomson viscoelastic material [42] (see also [38]). Then, we examine particular cases of SLSM.

The constitutive equation which relates the deviatoric tensors $\mathbf{s}^+$ and $\mathbf{e}^+$ in the material "+" is derived from the following relationships (see Fig. 3):

$$\mathbf{s}^+ = \mathbf{s}_1 + \mathbf{s}_2, \quad \mathbf{e}^+ = \mathbf{e}_1 = \mathbf{e}_2,$$
$$\mathbf{s}_1 = \mathbf{s}_1^e = \mathbf{s}^\eta, \quad \mathbf{e}_1 = \mathbf{e}_1^e + \mathbf{e}^\eta, \tag{3.11}$$
$$\mathbf{s}_1^e = 2\mu_1\mathbf{e}_1^e, \quad \mathbf{s}^\eta = 2\eta\dot{\mathbf{e}}^\eta, \quad \mathbf{s}_2 = 2\mu_2\mathbf{e}_2, \tag{3.12}$$

where μ_1 and μ_2 are the shear moduli of the elastic elements, η is the viscosity, $\mathbf{e}$ and $\mathbf{s}$ with various indices denote deviatoric strains and stresses in corresponding rheological elements, e.g., $\mathbf{s}_1^e$ is the deviatoric stress in the first elastic element, and $\mathbf{e}^\eta$ is the viscous deviatoric deformation. Finally, the constitutive equation takes the known form

$$\left(1 + \frac{\mu_2}{\mu_1}\right)\dot{\mathbf{e}}^+ + \frac{\mu_2}{\eta}\mathbf{e}^+ = \frac{1}{2\mu_1}\dot{\mathbf{s}}^+ + \frac{1}{2\eta}\mathbf{s}^+. \tag{3.13}$$

The strain energy of the constituents "+" is defined as

$$w_+ = \frac{1}{2}k_+(\vartheta^+ - \vartheta^{\mathrm{tr}})^2 + \mu_1\mathbf{e}_1^e : \mathbf{e}_1^e + \mu_2\mathbf{e}^+ : \mathbf{e}^+, \tag{3.14}$$

where it is taken into account that $\mathbf{e}_2 = \mathbf{e}^+$.

To find the strain energy w_+ at the reaction front, there is no need to solve complete viscoelastic problem. Indeed, viscous strains cannot occur at a point instantly when the front passes through it, while the transformation and elastic strains appear instantaneously. Therefore,

$$\mathbf{e}^\eta(y, t_y) = 0, \tag{3.15}$$

where t_y is the time at which the reaction front passes through the position having the coordinate y. It depends on y, and the dependence $t_y = t_y(y)$ is determined by the kinetics of the front propagation and follows from the equation

$$\int_0^{t_y} V(t)\mathrm{d}t = y. \tag{3.16}$$

Equation (3.15) will serve as an initial condition in the stress relaxation analysis, but now it is enough to know that from (3.15), it follows that at the reaction front $\mathbf{e}_1^e = \mathbf{e}^+$ and

$$\boldsymbol{\sigma}^+ = k_+ \left(\vartheta^+ - \vartheta^{\mathrm{tr}}\right) \mathbf{I} + 2\mu_+ \mathbf{e}^+, \tag{3.17}$$

$$w_+ = \frac{1}{2} k_+ (\vartheta^+ - \vartheta^{\mathrm{tr}})^2 + \mu_+ \mathbf{e}^+ : \mathbf{e}^+, \tag{3.18}$$

where $\mu_+ = \mu_1 + \mu_2$, and deviatoric strain $\mathbf{e}^+$ is taken at the reaction front.

Due to the plane strain restriction, $\varepsilon_y^+ = \vartheta^+ - \varepsilon_0$,

$$\mathbf{e}^+ : \mathbf{e}^+ = \boldsymbol{\varepsilon}^+ : \boldsymbol{\varepsilon}^+ - \frac{(\vartheta^+)^2}{3} = 2\left(\varepsilon_0^2 - \varepsilon_0 \vartheta^+ + \frac{(\vartheta^+)^2}{3}\right). \tag{3.19}$$

Thus, to calculate the strain energy w_+ it is enough to find the volume strain ϑ^+. From the relationships

$$\sigma_y^+ = k_+(\vartheta^+ - \vartheta^{\mathrm{tr}}) + 2\mu_+ e_y^+ = 0, \tag{3.20}$$

$$e_x^+ = \varepsilon_0 - \frac{\vartheta^+}{3}, \quad e_z^+ = -\frac{\vartheta^+}{3}, \quad e_y^+ = -(e_x^+ + e_z^+) = \frac{2\vartheta^+}{3} - \varepsilon_0, \tag{3.21}$$

it immediately follows that at the reaction front:

$$\vartheta^+ = \frac{3(2\mu_+ \varepsilon_0 + k_+ \vartheta^{\mathrm{tr}})}{3k_+ + 4\mu_+}, \tag{3.22}$$

$$e_x^+ = \frac{(3k_+ + 2\mu_+)\varepsilon_0 - k_+ \vartheta^{\mathrm{tr}}}{3k_+ + 4\mu_+}, \; e_y^+ = \frac{k_+(2\vartheta^{\mathrm{tr}} - 3\varepsilon_0)}{3k_+ + 4\mu_+}, \; e_z^+ = -\frac{2\mu_+ \varepsilon_0 + k_+ \vartheta^{\mathrm{tr}}}{3k_+ + 4\mu_+}. \tag{3.23}$$

The relationships (3.23) will be also used further in the stress relaxation analysis.

With the use of (3.22) and (3.19), the strain energy w_+ becomes a function of ε_0 and material parameters k_+, μ_+ and ϑ^{tr}. Then, the substitution of (3.8) for w_- and obtained expressions of w_+ and ϑ^+ into (2.11) gives χ as the quadratic function of external and transformation strains and elastic moduli of the constituents:

$$\chi(\varepsilon_0) = 2(G_+ - G_-)\varepsilon_0^2 - 3S\vartheta^{\mathrm{tr}}\varepsilon_0 + S(\vartheta^{\mathrm{tr}})^2, \tag{3.24}$$

where

$$G_\pm = \frac{\mu_\pm (3k_\pm + \mu_\pm)}{3k_\pm + 4\mu_\pm} = \frac{E_\pm}{4(1 - \nu_\pm^2)}, \quad S = \frac{2k_+\mu_+}{3k_+ + 4\mu_+} = \frac{E_+}{9(1 - \nu_+)}, \tag{3.25}$$

and $E_\pm$ and $\nu_\pm$ are the Young moduli and Poisson's ratios. Substitution of (3.24) into Eqs. (2.10) and (2.15) leads to the explicit dependencies of A_{NN} and c_{eq} on external and transformation strains, elastic moduli of the constituents and the chemical energies. In particular,

$$\frac{c_{\mathrm{eq}}}{c_*} = \exp\left\{-\frac{n_- M_-}{\rho_-} \frac{(\gamma - \chi(\varepsilon_0))}{RT}\right\}. \tag{3.26}$$

Note that at given ε_0, the equilibrium concentration does not depend on the front position. Then, the integration of the equation (3.4) leads to the kinetic equation in the form of the parabolic law:

$$\frac{T_{\mathrm{D}}}{2}\xi^2 + T_{\mathrm{ch}}\xi = Qt, \tag{3.27}$$

where

$$Q = \frac{n_- M_-}{\rho_-} c_*(1 - \phi), \phi = \frac{c_{\mathrm{eq}}}{c_*} = \exp\left\{-\frac{n_- M_-}{\rho_-} \frac{(\gamma - \chi(\varepsilon_0))}{RT}\right\} \tag{3.28}$$

(cf. with [34]).

By Eq. (3.27), the dependence (3.16) for $t_y(y)$, which is further substituted into (3.15), can be presented in the explicit form:

$$t_y = \frac{1}{Q}\left(\frac{T_{\mathrm{D}}}{2}\left(\frac{y}{H}\right)^2 + T_{\mathrm{ch}}\left(\frac{y}{H}\right)\right). \tag{3.29}$$

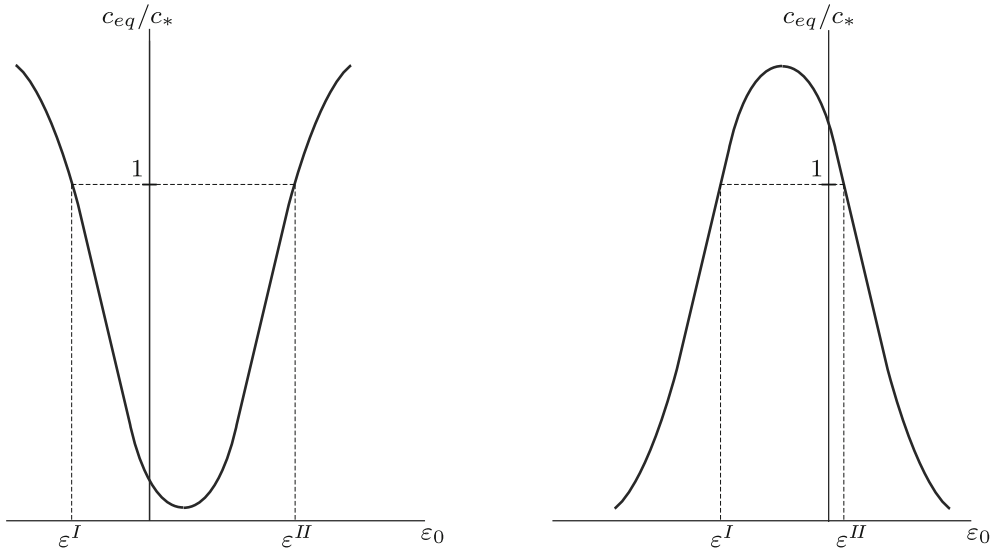

Fig. 4 Dependencies of the equilibrium concentration on the external strain: **a** $G_+ > G_-, \gamma > \gamma_*$, **b** $G_+ < G_-, \gamma_0 < \gamma < \gamma_*$

3.2 Equilibrium concentration, kinetics of the reaction front and blocking effect

In this section, the time dependencies of the reaction front position are examined finally at various values of the external strain ε_0, the energy parameter γ and the elastic moduli $k_\pm$, $\mu_\pm$ of solid constituents. Since, by (3.4), the reaction front velocity increases if $c_{\rm eq}/c_*$ decreases and, respectively, the velocity decreases if $c_{\rm eq}/c_*$ increases, the influence of various parameters on the reaction front behavior can be predicted qualitatively if one knows how the parameters affect the equilibrium concentration. So, we start with such predictions.

By (3.4), the reaction front can propagate only if the stress–strain state at the front and the energy parameter are such that $c_{\rm eq} < c_*$. We study further how the condition $c_{\rm eq} < c_*$ is affected by the parameters. By (3.26), this is possible only if the transformation strain, external strains, elasticity parameters and the energy parameter are such that $\chi < \gamma$ [9,15]. By (3.24), in the considered case this condition takes the form

$$\chi(\varepsilon_0) - \gamma = 2(G_+ - G_-)\varepsilon_0^2 - 3S\vartheta^{\rm tr}\varepsilon_0 - (\gamma - \gamma_0) < 0, \tag{3.30}$$

where

$$\gamma_0 = S(\vartheta^{\rm tr})^2 \tag{3.31}$$

is the critical value of the parameter γ in the sense that the reaction front may propagate at the external strain $\varepsilon_0 = 0$ only if

$$\gamma > \gamma_0.$$

Formula (3.31) for the critical value of γ for the plane transformation strain with slightly different S was presented in [11,15] for the case of elastic reaction constituents. The same formula appears here because of the pure elastic behavior of both constituents at the front at the transformation moment t_y.

The dependencies of $c_{\rm eq}/c_*$ on external strain ε_0 for the planar front are schematically shown in Fig. 4. The extrema are reached at $\varepsilon_0 = \varepsilon_0^*$ with $c_{\rm eq}/c_* = c_{\rm eq}^*/c_*$ where

$$\frac{c_{\rm eq}^*}{c_*} = \exp\left\{\frac{n_- M_-}{\rho_-}\frac{(\chi(\varepsilon_0^*) - \gamma)}{RT}\right\},$$
$$\varepsilon_0^* = \frac{3S\vartheta^{\rm tr}}{4(G_+ - G_-)}, \qquad \chi(\varepsilon_0^*) = \left(1 - \frac{9S}{8(G_+ - G_-)}\right)\gamma_0 \equiv \gamma_*. \tag{3.32}$$

Note that $\varepsilon_0^* \neq 0$, since k_+ and μ_+ are positive values.

The character of the dependence of c_{eq}/c_* on ε_0 and the signs of ε_0^* and $\chi(\varepsilon_0^*)$ depend on the relation between G_+, G_- and S and the sign of the transformation strain ϑ^{tr}. Without loss of generality, we assume further that $\vartheta^{tr} > 0$. As for the elastic moduli, in accordance with (3.32), the following three cases can be distinguished for which different influences of the external strain on the front propagation can be observed.

(i) If

$$8(G_+ - G_-) - 9S > 0, \tag{3.33}$$

then $G_+ > G_-$ and, therefore, $\chi(\varepsilon_0^*) > 0$ and $\varepsilon_0^* > 0$ correspond to the minimal value of $\chi(\varepsilon_0)$ as it is shown in Fig. 4a. Note that the inequality (3.33) can be rewritten through elastic moduli as

$$\mu_+ > \frac{4\mu_-(3k_- + \mu_-)}{3k_- + 4\mu_-} \iff \frac{E_+}{1+\nu_+} > \frac{2E_-}{1-\nu_-^2}.$$

The front can propagate only if the energy parameter, elastic moduli of the solid constituents and transformation strain are such that $\gamma > \gamma_*$ and only at strains $\varepsilon_0 \in [\varepsilon^I, \varepsilon^{II}]$ where ε^I, ε^{II} are the roots of the quadratic equation $\chi(\varepsilon_0) - \gamma = 0$. If $\gamma_* < \gamma < \gamma_0$, then both roots are positive and the front cannot propagate without applied tensile strain $\varepsilon_0 > \varepsilon^I > 0$.

If the front propagates at $\varepsilon_0 = 0$, then $\gamma > \gamma_0$ and the roots have different signs, $\varepsilon^I < 0$ and $\varepsilon^{II} > 0$. The propagation is blocked starting from some strains in both tension at $\varepsilon_0 > \varepsilon^{II}$ and compression at $\varepsilon_0 < \varepsilon^I$.

If the energy parameter $\gamma < \gamma_*$, then $c_{eq}/c_* > 1$ at all ε_0, and the planar front cannot propagate in y-direction. To avoid misunderstanding, note that this does not mean that the reaction cannot occur at all. In a general case, χ depends on the geometry of the front since the stress–strain state at the reaction front depends on the geometry. It may happen that other configurations of the reaction front than a configuration with a planar reaction front may develop. On the other hand, a forbidden zone can be constructed in a strain space, formed by the strains at which the reaction cannot go whatever the local normals to the front are [11,13]. Also, strictly speaking, even if the considered solution with a planar propagating front is allowed by kinetic equation at given ε_0, an additional stability analysis would be appropriate [35]. Consideration of these aspects is beyond the scope of this paper. Note only that the use of the semi-inverse approach may give a mathematically consistent solution, but other solutions which do not follow a priori assumptions about the geometry of the front may also be of interest.

(ii) If the elastic moduli satisfy the inequalities

$$G_+ > G_- \quad \text{but} \quad 8(G_+ - G_-) - 9S < 0,$$

which can be rewritten as

$$\mu_+ < \frac{4\mu_-(3k_- + \mu_-)}{3k_- + 4\mu_-} < \frac{4\mu_+(3k_+ + \mu_+)}{3k_+ + 4\mu_+} \iff \frac{E_+}{2(1+\nu_+)} < \frac{E_-}{1-\nu_-^2} < \frac{E_+}{1-\nu_+^2},$$

then $\varepsilon_0^* > 0$ as in the case (i), but the minimal value of χ is negative, $\chi(\varepsilon_0^*) < 0$. The front may propagate even at negative jump of the chemical energies, $\gamma < 0$, but such that $\gamma > -|\gamma_*|$, and at strains ε_0 such that $\chi(\varepsilon_0^*) < \chi(\varepsilon_0) < \gamma < 0$. This would be impossible without accounting for strain energy effects.

Since $\varepsilon_0^* > 0$ at $G_+ > G_-$, the increase of the tensile strain from $\varepsilon_0 = 0$ until ε_0^* accelerates the reaction front in both cases (i) and (ii). Further growth of ε_0 retards the front until blocking at ε^{II}. On the whole, if $|\varepsilon_0 - \varepsilon_0^*|$ increases, then the front velocity decreases until zero.

(iii) If $G_+ < G_-$, then $\gamma_0 < \gamma_*$, $\varepsilon_0^* < 0$, and $\chi(\varepsilon_0^*) > 0$ corresponds to the maximal value on the dependence $\chi(\varepsilon_0)$ (Fig. 4b). Such a case was also discussed for an elastic case with plane transformation strain in [15]. If $\gamma > \gamma_*$, then the front may propagate at any ε_0. If $\gamma < \gamma_*$, then the front is blocked at $\varepsilon_0 \in [\varepsilon^I, \varepsilon^{II}]$ but may start to propagate at proper tension $\varepsilon_0 > \varepsilon^{II}$ or compression $\varepsilon_0 < \varepsilon^I$. Thus, in this case, in contrast to the previous ones, the front may propagate at any γ at some external strains.

By (3.32), the bulk and shear elastic moduli, $k_\pm$ and $\mu_\pm$, affect the dependence $\chi(\varepsilon_0)$ and, thus, the dependencies of c_{eq}/c_* and the reaction front velocity on ε_0 via parameters $(G_+ - G_-)$ and S, and the strain ε_0^* is determined by the dimensionless parameter $S/(G_+ - G_-)$. For example, it is easy to see that ε_0^* decreases if μ_+ increases and other moduli are fixed. As another example, one can examine how k_+ affects the dependence $\chi(\varepsilon_0)$ and the extrema values $\chi(\varepsilon_0^*)$ and ε_0^*. From (3.24), it follows that

$$\frac{\partial \chi(\varepsilon_0)}{\partial k_+} = \frac{2\mu_+^2(3\varepsilon_0 - 2\vartheta^{tr})^2}{(3k_+ + 4\mu_+)^2} \geq 0. \tag{3.34}$$

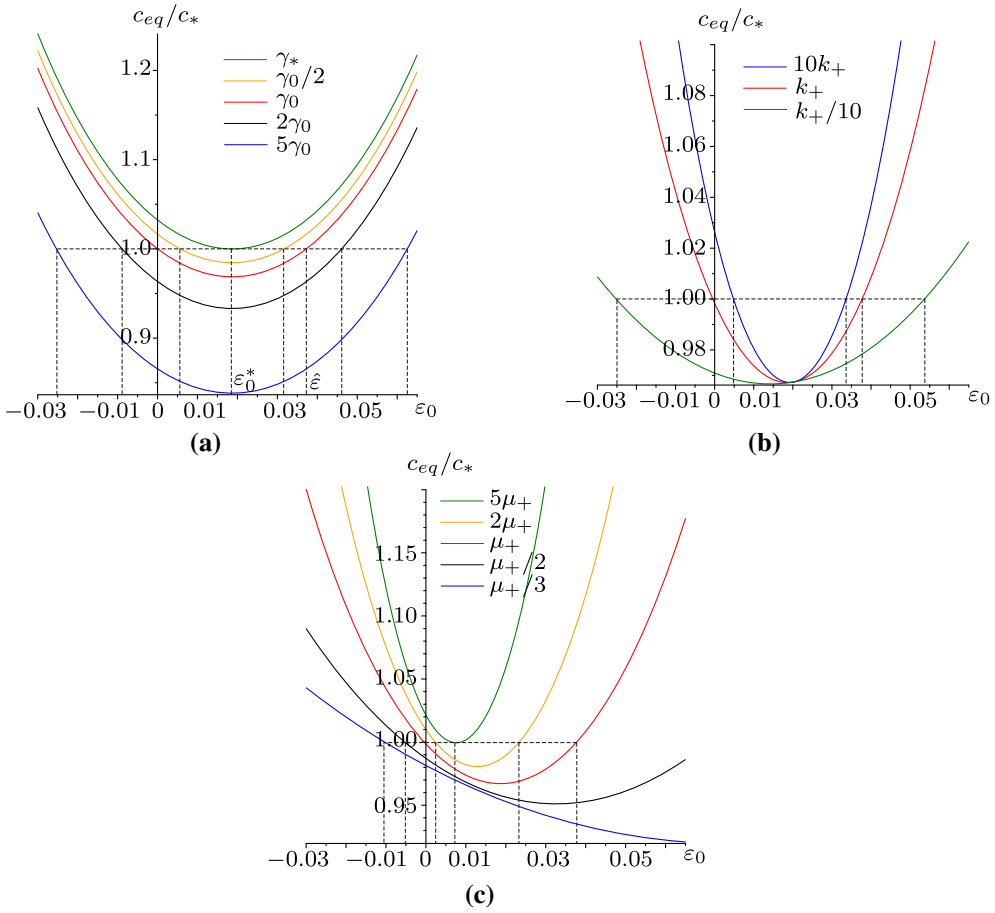

Fig. 5 Dependencies of the equilibrium concentration on external strain ε_0 for the case $G_+ > G_-$: **a** for different values of the energy parameter γ; **b** for different values of the bulk modulus k_+; **c** for different values of the shear modulus μ_+

Then, if the front propagates at a given set of parameters, further increase of k_+ increases $\chi(\varepsilon_0)$ and, therefore, decreases the front velocity. Note also that increase of k_+ leads to increasing the extrema value $\chi(\varepsilon_0^*)$ for both cases $G_+ > G_-$ and $G_+ < G_-$.

By (3.32), the character of the dependence of the extrema strain ε_0^* on the bulk modulus k_+ depends on the relations between elastic moduli. Since

$$\frac{\partial \varepsilon_0^*}{\partial k_+} = \frac{3\mu_+^2 \vartheta^{\mathrm{tr}}}{(3k_+ + 4\mu_+)^2} \frac{8(G_+ - G_-) - 9S}{4(G_+ - G_-)^2}, \tag{3.35}$$

one can see that if $8(G_+ - G_-) - 9S > 0$ (the case (i)), then the point ε_0^* in Fig. 4a is shifted to the right if k_+ increases and is shifted to the left leaving ε_0^* positive if k_+ decreases, respectively.

If $G_+ > G_-$ but $8(G_+ - G_-) - 9S < 0$ (the case (ii)) or $G_+ < G_-$ (the case (iii)), then the extrema point ε_0^* in Fig. 4a is shifted to the left or right if k_+ increases or decreases, respectively.

More detailed quantitative analysis is presented in Figs. 5 and 6, where the dependencies of the relative equilibrium concentration c_{eq}^*/c_* on the external stain ε_0 at various values of the energy parameter γ and the bulk and shear modules k_+, μ_+ of the transformed material are shown for the cases $G_+ > G_-$ and $G_+ < G_-$, respectively. The reference values of the parameters for the cases $G_+ > G_-$ and $G_+ < G_-$ and corresponding values of γ_0, γ_* and G_+, G_-, S are given in Tables 1 and 2, respectively. Only the parameters differ in two cases which are shown in Table 2. If the parameter is varied, then the values are indicated in figures.

The choice of the values of the parameters was made according to the reasons of the consistency with a small strain approach, wide range of values and better visualization of the parameters influence on the variety of the reaction front behavior in dependence on external strain. Two sets of bulk and shear moduli, $k_\pm$ and $\mu_\pm$, were taken which correspond to the cases $G_+ > G_-$ (Figs. 5, 7, 8, 9, 10) and $G_+ < G_-$ (Fig. 6).

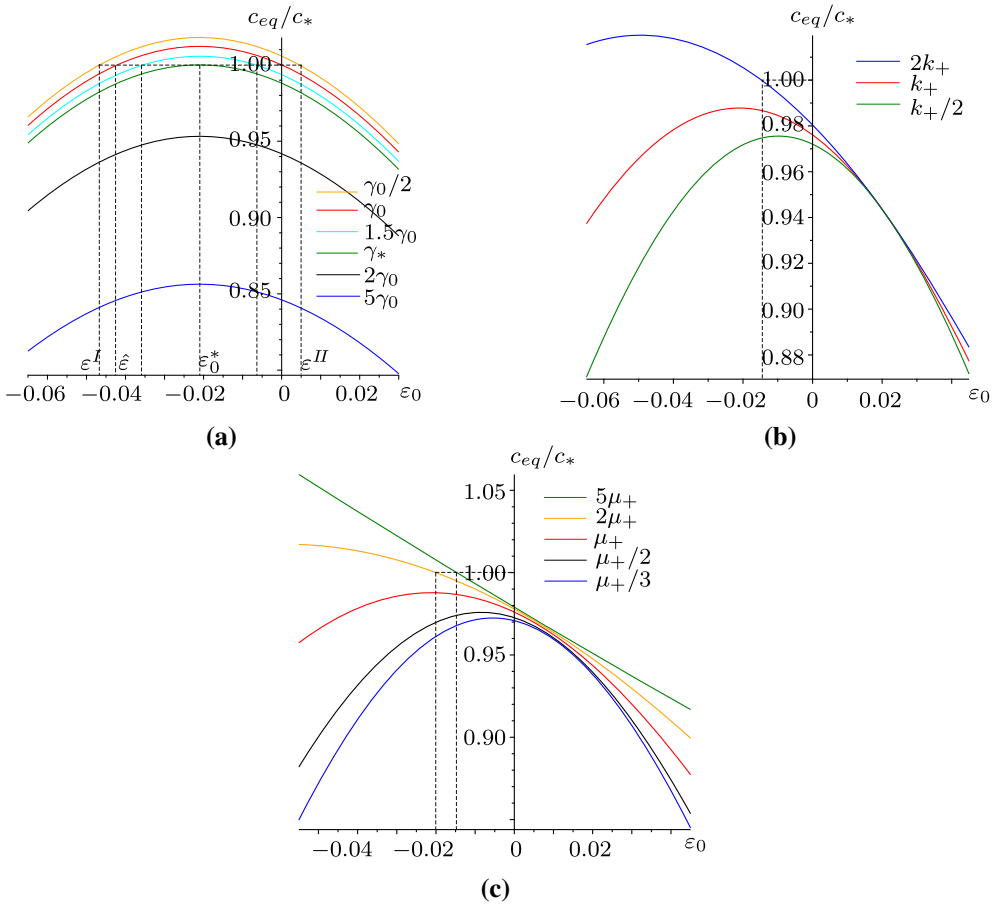

Fig. 6 Dependencies of the equilibrium concentration on external strain ε_0 for the case $G_+ < G_-$: **a** for different values of the energy parameter γ; **b** for different values of the bulk modulus k_+; **c** for different values of the shear modulus μ_+

Table 1 Material parameters used in the simulations for the case $G_+ > G_-$

Parameter	k_- [GPa]	μ_- [GPa]	k_+ [GPa]	μ_+ [GPa]	ϑ^{tr}
Value	27.3	25.9	90.9	67.7	0.03
Parameter	γ [MJ/m^3]	γ_0 [MJ/m^3]	γ_* [MJ/m^3]	η_0 [GPa s]	D [m^2/s]
Value	42.9	20.4	14.03	15.9	8×10^{-10}
Parameter	α [m/s]	k_* [m/s]	T [K]	c_* n_-	H [m]
Value	2.3×10^{-7}	1.27×10^{-6}	920	1 1	10^{-3}
Parameter	M_- [g/mol]	ρ_- [g/cm^3]	G_- [GPa]	G_+ [GPa]	S [GPa]
Value	28.1	15	15	42.6	22.6

Table 2 Material parameters used in the simulations for the case $G_+ < G_-$

Parameter	k_- [GPa]	μ_- [GPa]	k_+ [GPa]	μ_+ [GPa]	γ [MJ/m^3]
Value	62.3	33.9	27.3	25.9	21.9
Parameter	γ_0 [MJ/m^3]	γ_* [MJ/m^3]	G_- [GPa]	G_+ [GPa]	S [GPa]
Value	6.86	14.04	23.2	15	7.6

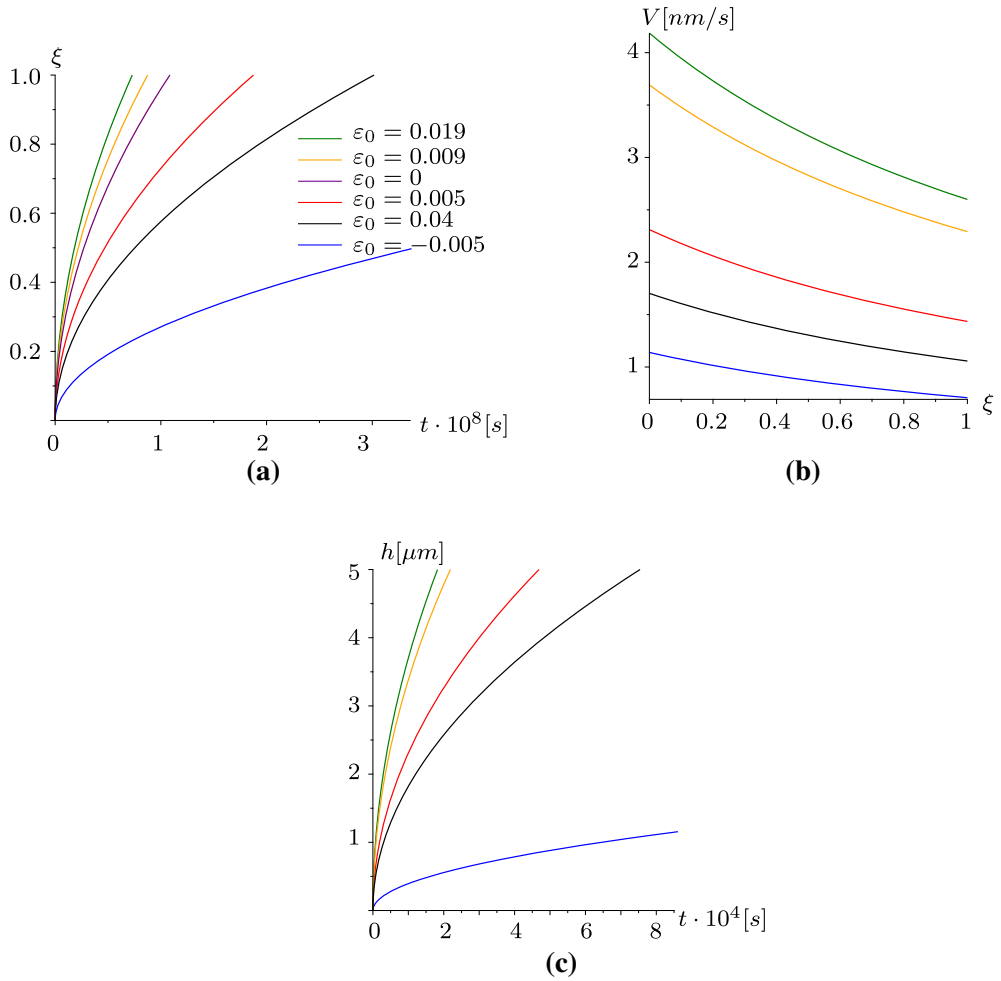

Fig. 7 Kinetics of the reaction front at various values of external tension ε_0 for the case $G_+ > G_-$: **a** dependencies of the dimensionless front position on time, **b** dependencies of the front velocity on the position, **c** the front position versus time at the initial stage of the front propagation

We took $c_* = 1$ for the sake of simplicity, implying that the concentration of the diffusing constituent may be considered in dimensionless form, divided by the solubility c_*. Note that the dimensionless forms of the current and equilibrium concentrations are consistent with Eqs. (3.1)–(3.3) and (3.26) defining the concentrations.

Figures 5a and 6a reflect the competition between strain and chemical energies at $G_+ > G_-$ and $G_+ < G_-$, respectively. If $\gamma = \gamma_0$, then the dependence of $c_{\rm eq}/c_*$ on ε_0 passes through the point $\varepsilon_0 = 0$, $c_{\rm eq}/c_* = 1$. If $G_+ > G_-$ and $\gamma = \gamma_0$, then the front may propagate only at tension restricted by the strain $\hat{\varepsilon} = 3S\vartheta^{\rm tr}/[2(G_+ - G_-)]$, i.e., at strains $0 < \varepsilon_0 < \hat{\varepsilon}$ ($\hat{\varepsilon} = 0.037$ in Fig. 5a). One can see how increasing γ results in enlarging the interval of allowed strains ε_0 (see the curves for $\gamma = 2\gamma_0$ and $\gamma = 5\gamma_0$) and how the decrease of γ shortens and shifts the interval of the strains at $\gamma_* < \gamma < \gamma_0$.

If $G_+ < G_-$ and $\gamma = \gamma_0$, then the front may propagate only at tension $\varepsilon_0 > 0$ or compression $\varepsilon_0 < \hat{\varepsilon} = -0.042$ (Fig. 6a). If $\gamma < \gamma_0$, for example, $\gamma = \gamma_0/2$, then the front can propagate only if additional tension $\varepsilon_0 > \varepsilon^{II} > 0$ or compression $\varepsilon_0 < \varepsilon^{I} < 0$ is applied. The case $\gamma_0 < \gamma < \gamma_*$ is presented by $\gamma = 1.5\gamma_0$, and the front propagation is blocked at $\varepsilon_0 \in [-0.036, -0.006]$. If $\gamma > \gamma_*$ ($\gamma = 2\gamma_0$ and $\gamma = 5\gamma_0$ in Fig. 6a), then the front may propagate at any ε_0.

One can also see in Figs. 4b, and 6a that if, at $G_+ < G_-$, the front can propagate at some ε_0, then further increase of the absolute value $|\varepsilon_0|$ decreases $c^*_{\rm eq}/c_*$ and, thus, increases the front velocity.

Figures 5b, c and 6b, c characterize quantitatively the role of volume and shear strain energies via the influence of the bulk modulus k_+ and shear modulus μ_+ on the dependencies of $c^*_{\rm eq}/c_*$ on ε_0.

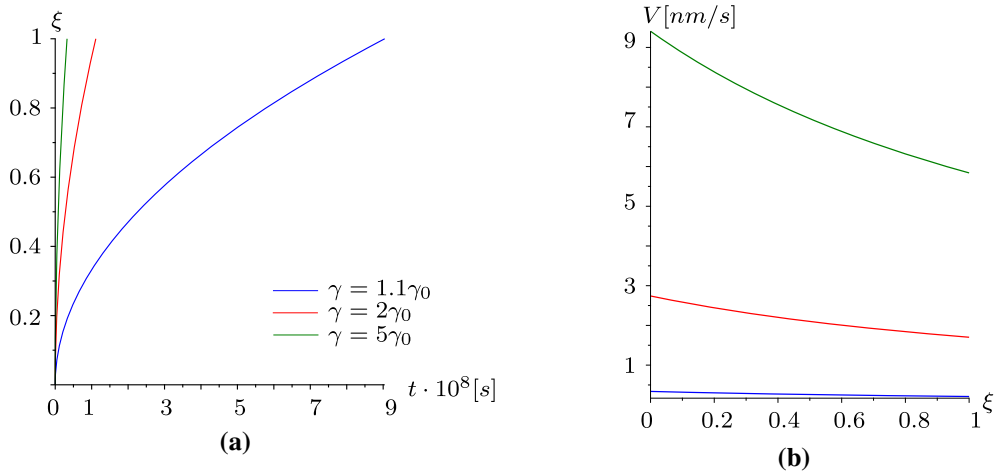

Fig. 8 Dependencies of the front position on time (**a**), and the front velocity on the position (**b**) at various values of energy parameter γ ($G_+ > G_-$)

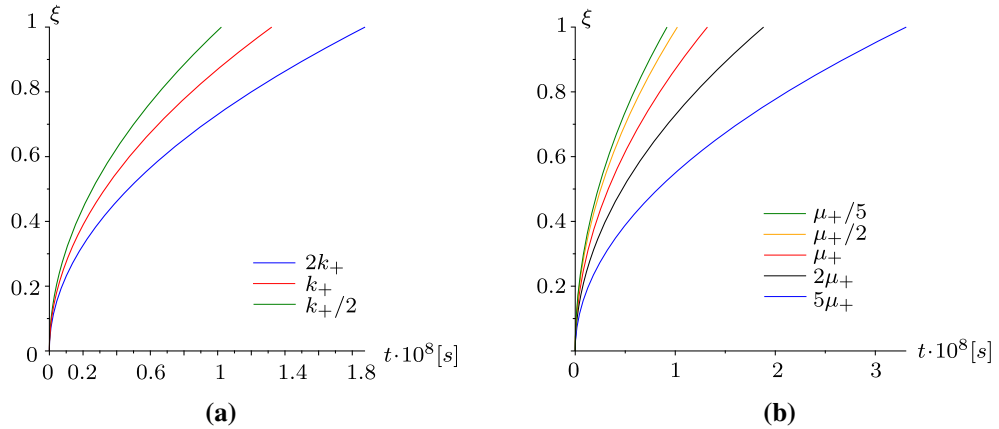

Fig. 9 Dependencies of the front position on time: **a** at various values of the bulk modulus k_+, **b** at various values of the shear modulus μ_+ ($G_+ > G_-$)

Since G_+ decreases and, thus, approaches to G_- if μ_+ decreases and $G_+ > G_-$, then one can also observe in Fig. 5c how the dependence of c_{eq}/c_* on external strain changes if $G_+ \to G_-$. (The curves move to right and straighten up.) Analogously, Fig. 6c demonstrates how the dependencies change at $G_+ < G_-$ if G_+ increases and approaches to G_- if μ_+ increases.

Corresponding dependencies of the front position on time and the front velocity on the position under various ε_0 for the case $G_+ > G_-$ are shown in Fig. 7. One can see how the strains retard or accelerate the reaction front. The maximal velocity is observed at tensile strain $\varepsilon_0 = \varepsilon_0^* = 0.019$. The velocity decreases at both additional tension (as at $\varepsilon_0 = 0.04$) and at compression relatively to ε_0^* (as at $\varepsilon_0 = 0.005, 0.009, -0.005$), as it has to be in accordance with the increasing c_{eq}/c_* in Fig. 5a.

Figures 8 and 9 demonstrate how increase of the energy parameter accelerates the front, and how the values of elastic moduli affect the front kinetics. These dependencies are consistent with the dependencies of c_{eq}/c_* shown in Fig. 5.

The initial thickness of the plate also has an effect on the front kinetics (Fig. 10) through characteristic times T_{D} and T_{ch} of the diffusion supply and chemical reaction (see Eq. (3.5)). Increasing the plate thickness increases the characteristic times and therefore decreases the relative front velocity.

Kinetic curves analogous to the dependencies shown in Figs. 7, 8, 9 and 10 can be constructed at $G_+ < G_-$, and finally, we illustrate how the sign of the difference $G_+ - G_-$ and the value of the parameter S affect the reaction front kinetics (Fig. 11). By (3.27), (3.28) and (3.24), the elastic moduli and external strain affect the

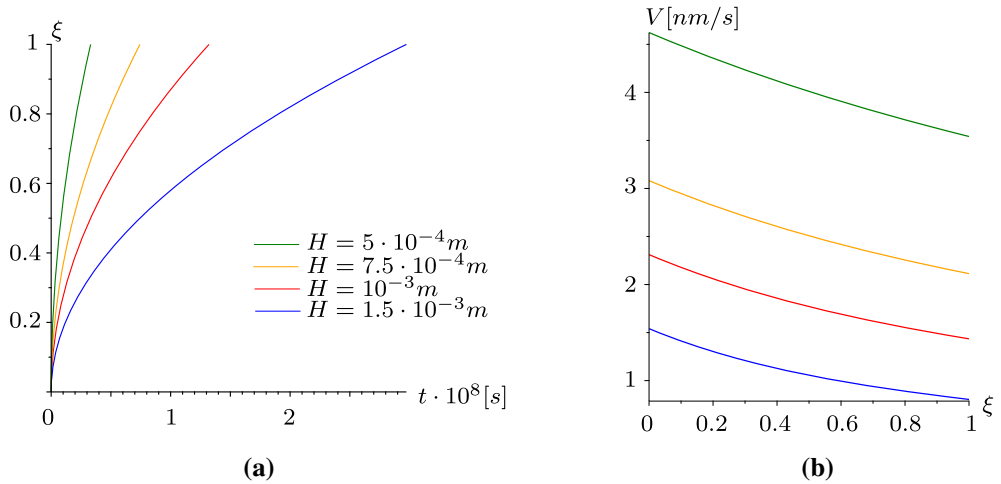

Fig. 10 **a** Dependencies of the front position on time, **b** dependencies of the front velocity on the position at various initial thickness H of the plate ($G_+ > G_-$)

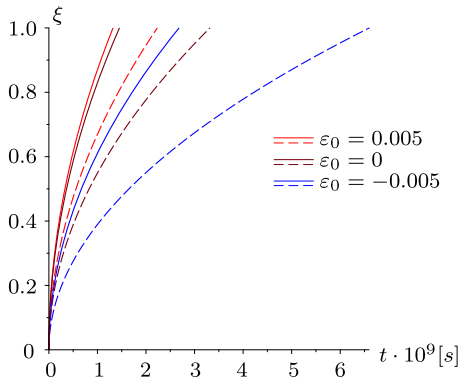

Fig. 11 Kinetics of the reaction front at various values of external tension ε_0 for the case $G_+ > G_-$ (solid lines) and for the case $G_+ < G_-$ (dashed lines)

parabolic kinetic via the influence on the coefficient Q, i.e., via changing the timescale due to changing the parameters S and the difference $G_+ - G_-$.

If $\varepsilon_0 = 0$, then, by (3.24), $\chi(\varepsilon_0) = S(\vartheta^{\rm tr})^2$ in (3.28), and the difference $G_+ - G_-$ itself does not affect the front kinetics. The front propagates slower in the case $G_+ < G_-$ only because the value S is smaller in this case than in the case of $G_+ > G_-$ at taken elastic moduli (see Tables 1, 2). Recall that S is defined by the elastic moduli of the transformed material only.

One can also compare quantitatively how the external strain affects the kinetics if the elastic moduli are such that $G_+ > G_-$ or $G_+ < G_-$. In particular, the front propagates at $G_+ < G_-$ slower than at $G_+ > G_-$ as it was due to the different values of S, but compared to the case $\varepsilon_0 = 0$, the difference is greater at compression and smaller at tension.

3.3 Stress relaxation and strains behind the reaction front

To calculate stresses and strains in the transformed material, i.e., behind the reaction front, according to Eqs. (3.9)–(3.12) one has to calculate the time evolution of volume strain ϑ^+ and deviators $\mathbf{e}_2 = \mathbf{e}^+$, $\mathbf{e}^\eta$, $\mathbf{e}_1^e$.

Substitution of $\boldsymbol{\varepsilon}^+ - \frac{\vartheta^+}{3}\mathbf{I}$ and $\boldsymbol{\sigma}^+ - \sigma^+\mathbf{I}$ into Eq. (3.13) instead of $\mathbf{s}^+$ and $\mathbf{e}^+$ with the restrictions $\varepsilon_x^+ = \varepsilon_0$, $\varepsilon_z^+ = 0$, leads to the equations

$$-\left(1+\frac{\mu_2}{\mu_1}\right)\frac{\dot\vartheta^+}{3} + \frac{\mu_2}{\eta}\left(\varepsilon_0 - \frac{\vartheta^+}{3}\right) = \frac{1}{2\mu_1}\left(\dot\sigma_x^+ - \dot\sigma^+\right) + \frac{1}{2\eta}(\sigma_x^+ - \sigma^+), \tag{3.36}$$

$$-\left(1+\frac{\mu_2}{\mu_1}\right)\frac{\dot\vartheta^+}{3} - \frac{\mu_2}{\eta}\frac{\vartheta^+}{3} = \frac{1}{2\mu_1}\left(\dot\sigma_z^+ - \dot\sigma^+\right) + \frac{1}{2\eta}(\sigma_z^+ - \sigma^+). \tag{3.37}$$

Adding Eqs. (3.36) and (3.37) and taking into account Eq. (3.10), we derive the differential equation for ϑ^+:

$$\dot\vartheta^+ + \frac{\vartheta^+}{\tau_+} - \frac{3(k_+\vartheta^{\rm tr} + 2\mu_2\varepsilon_0)}{\tau_1\,(3k_+ + 4\mu_+)} = 0, \tag{3.38}$$

where

$$\tau_1 = \frac{\eta}{\mu_1}, \quad \tau_+ = \frac{(3k_+ + 4\mu_+)}{(3k_+ + 4\mu_2)}\frac{\eta}{\mu_1}. \tag{3.39}$$

The initial condition for Eq. (3.38) is the value $\vartheta^+(t_y)$ at time t_y; it is given by (3.22). Then, the solution of Eq. (3.38) takes the form:

$$\vartheta^+(y,t) = a\exp\left(-\frac{t-t_y}{\tau_+}\right) + b, \tag{3.40}$$

where

$$a = \frac{2\beta\mu_1 k_+}{3k_+ + 4\mu_+}(3\varepsilon_0 - 2\vartheta^{\rm tr}), \quad b = \beta\vartheta^{\rm tr} + \frac{6\mu_2\varepsilon_0}{3k_+ + 4\mu_2}, \tag{3.41}$$

$$\beta = \left(1 + \frac{4\mu_2}{3k_+}\right)^{-1}, \tag{3.42}$$

and the time $t_y = t_y(y)$ is given by (3.29). Note that here $t > t_y$, and the coordinate y is presented in $t_y(y)$ in a dimensionless form as $\zeta = y/H \in [0,\xi]$. One can see that the volume strain in points behind the front decreases or increases with time depending on the sign of the difference $(3\varepsilon_0 - 2\vartheta^{\rm tr})$.

Next steps are finding e_x^+, e_{1x}^e and then

$$\sigma_x^+ = k_+(\vartheta_+ - \vartheta^{\rm tr}) + 2\mu_1 e_{1x}^e + 2\mu_2 e_x^+, \tag{3.43}$$

$$\sigma_z^+ = 3k_+(\vartheta^+ - \vartheta^{\rm tr}) - \sigma_x^+. \tag{3.44}$$

Since $e_x^+ = \varepsilon_0 - \vartheta^+/3$, it follows from (3.40) that

$$e_x^+(y,t) = \frac{2\beta\mu_1}{3k_+ + 4\mu_+}\left(\frac{2\vartheta^{\rm tr}}{3} - \varepsilon_0\right)\exp\left(-\frac{t-t_y}{\tau_+}\right) + \frac{3k_+ + 2\mu_2}{3k_+ + 4\mu_2}\varepsilon_0 - \frac{\beta\vartheta^{\rm tr}}{3}. \tag{3.45}$$

By constitutive equations (3.12),

$$\mathbf{e}_1^e = \tau_1\dot{\mathbf{e}}^\eta = \tau_1(\dot{\mathbf{e}}^+ - \dot{\mathbf{e}}_1^e).$$

Then, since $\dot e_x^+ = -\dot\vartheta^+/3$, it follows that e_{1x}^e can be found from the equation

$$\dot e_{1x}^e + \frac{1}{\tau_1}e_{1x}^e = -\frac{\dot\vartheta^+}{3} \tag{3.46}$$

with the initial condition

$$e_{1x}^e(y,t_y) = e_x^+(y,t_y) = \varepsilon_0 - \frac{\vartheta^+(y,t_y)}{3} \tag{3.47}$$

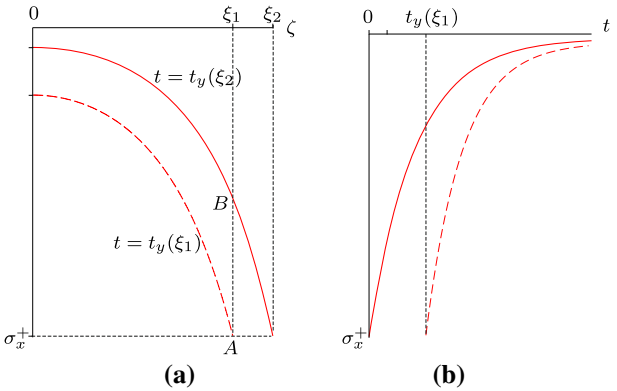

Fig. 12 Stress relaxation behind the reaction front: **a** stress distributions behind the front for two front positions at times $t = t_y(\xi_1)$ and $t = t_y(\xi_2)$; **b** stress relaxation in points $\zeta = 0$ and $\zeta = \xi_1$ starting from the moments $t = t_y(0) = 0$ and $t = t_y(\xi_1)$, respectively

that follows from Eq. (3.15) with $\vartheta^+(y, t_y)$ defined by Eq. (3.22).

After calculating the time derivative $\dot{\vartheta}^+$ from Eq. (3.40) and substituting it into the right-hand side of Eq. (3.46), we come to the equation for e^e_{1x} that, with the initial condition (3.47), has a solution:

$$e^e_{1x}(y,t) = \frac{k_+(3\varepsilon_0 - 2\vartheta^{\rm tr})}{2(3k_+ + 4\mu_+)} \exp\left(-\frac{t-t_y}{\tau_+}\right) + \frac{\varepsilon_0}{2} \exp\left(-\frac{t-t_y}{\tau_1}\right). \tag{3.48}$$

Finally, from (3.43), (3.40), (3.45) and (3.48) it follows that

$$\begin{aligned}\sigma_x^+(y,t) = {} & \frac{3\beta\mu_1 k_+ \left(3\varepsilon_0 - 2\vartheta^{\rm tr}\right)}{3k_+ + 4\mu_+} \exp\left(-\frac{t-t_y}{\tau_+}\right) \\ & + \mu_1\varepsilon_0 \exp\left(-\frac{t-t_y}{\tau_1}\right) + \frac{4\mu_2(3k_+ + \mu_2)\varepsilon_0}{3k_+ + 4\mu_2} - 2\beta\mu_2\vartheta^{\rm tr},\end{aligned} \tag{3.49}$$

$$\begin{aligned}\sigma_z^+(y,t) = {} & \frac{3\beta\mu_1 k_+ \left(3\varepsilon_0 - 2\vartheta^{\rm tr}\right)}{3k_+ + 4\mu_+} \exp\left(-\frac{t-t_y}{\tau_+}\right) \\ & - \mu_1\varepsilon_0 \exp\left(-\frac{t-t_y}{\tau_1}\right) + \frac{2\mu_2(3k_+ - 2\mu_2)\varepsilon_0}{3k_+ + 4\mu_2} - 2\beta\mu_2\vartheta^{\rm tr}\end{aligned} \tag{3.50}$$

Then, at the reaction front

$$\sigma_x^+(y,t_y) = \frac{2\mu_+\left(2(3k_+ + \mu_+)\varepsilon_0 - 3k_+\vartheta^{\rm tr}\right)}{3k_+ + 4\mu_+}, \tag{3.51}$$

$$\sigma_z^+(y,t_y) = \frac{2\mu_+\left((3k_+ - 2\mu_+)\varepsilon_0 - k_+\vartheta^{\rm tr}\right)}{3k_+ + 4\mu_+} \tag{3.52}$$

The distributions of stress σ_x^+ behind the reaction front at two moments $t_y(y)$ which correspond to the front positions $\xi_1 = y_1/H$ and $\xi_2 = y_2/H$ are schematically shown in Fig. 12a. The stress σ_x^+ in the point $\zeta = \xi_1$ relaxes from A to B during the time of the front propagation from ξ_1 to ξ_2. Stress relaxation in two points $\zeta = 0$ and $\zeta = \xi_1$ starting from the moments $t = t_y(0) = 0$ and $t = t_y(\xi_1)$, respectively, is shown in Fig. 12b.

The relaxation of stress σ_x becomes possible because the viscous deformations convert the volume expansion $\vartheta^{\rm tr}$ into the strain ε_y^+, i.e., thickening of the transformed layer. The dependence $\varepsilon_y^+(y,t)$ follows from the equality

$$\varepsilon_y^+ = \vartheta^+ - \varepsilon_0 \tag{3.53}$$

where ϑ^+ is determined by (3.40).

To find inputs of viscous strain $\mathbf{e}^{\eta}$ and elastic part $\mathbf{e}_1^e$, note that it follows from (3.11), (3.12) that

$$\mathbf{e}^{\eta} = \left(1 + \frac{\mu_2}{\mu_1}\right)\mathbf{e}^{+} - \frac{1}{2\mu_1}\left(\boldsymbol{\sigma}^{+} - \sigma^{+}\mathbf{I}\right). \tag{3.54}$$

Then, with $e_y^{+} = \frac{2}{3}\vartheta^{+} - \varepsilon_0$ (see (3.21)) and $\sigma_y = 0$, $\sigma_{+} = k_{+}(\vartheta^{+} - \vartheta^{\mathrm{tr}})$, it follows from (3.54) that

$$e_y^{\eta}(y,t) = \frac{1}{2\mu_1}\left\{\left(k_{+} + \frac{4}{3}\mu_{+}\right)\vartheta^{+}(y,t) - \left(k_{+}\vartheta^{\mathrm{tr}} + 2\mu_{+}\varepsilon_0\right)\right\}, \tag{3.55}$$

By (3.11), $\mathbf{e}_1^e = \mathbf{e}^{+} - \mathbf{e}^{\eta}$. Then,

$$e_{1y}^{e}(y,t) = \frac{1}{2\mu_1}\left\{k_{+}\vartheta^{\mathrm{tr}} - \left(k_{+} + \frac{4}{3}\mu_2\right)\vartheta^{+}(y,t) + 2\mu_2\varepsilon_0\right\}. \tag{3.56}$$

In Eqs. (3.55) and (3.56), the dependence $\vartheta^{+}(y,t)$ is given by (3.40).

If $\varepsilon_0 = 0$, then strains and stresses are sourced only by the transformation strain, and due to the relaxation at $t \to \infty$

$$\varepsilon_y^{+} = \vartheta^{+} \to \beta\vartheta^{\mathrm{tr}}, \quad e_y^{\eta} \to 2\beta\vartheta^{\mathrm{tr}}/3, \quad e_{1y}^{e} \to 0, \tag{3.57}$$

$$e_{1x}^{e} \to 0, \quad e_x^{+} \to e_x^{\eta} = -\beta\vartheta^{\mathrm{tr}}/3, \quad \sigma_x^{+} \to -2\mu_2\beta\vartheta^{\mathrm{tr}}, \tag{3.58}$$

and one can see that the coefficient β, defined by (3.42), characterizes the degree of the conversion of the transformations strain into ε_y^{+} and the value of the residual compressive stress σ_x^{+}.

The strain ε_y^{+} may be also of interest, since in experiments the thickness of the layer of the transformed material is usually observed which does not coincide with the coordinate h of the front position. To estimate the thickness, one have to add to h the displacements produced by strains $\varepsilon_y^{+}(y)$ at $y \in [0,h]$, i.e., to calculate the integral

$$\begin{aligned}\int_0^h \varepsilon_y^{+}(y)\mathrm{d}y &= \int_0^h (\vartheta^{+}(y,t_h) - \varepsilon_0)\mathrm{d}y \\ &= a\int_0^h \exp\left(\frac{t_y - t_h}{\tau_{+}}\right)\mathrm{d}y + (b - \varepsilon_0)h,\end{aligned} \tag{3.59}$$

where t_h is the moment of observation of the front position h, and, by (3.29),

$$t_y = \frac{1}{Q}\left(\frac{T_{\mathrm{D}}}{2}\zeta^2 + T_{\mathrm{ch}}\zeta\right), \quad t_h = \frac{1}{Q}\left(\frac{T_{\mathrm{D}}}{2}\xi^2 + T_{\mathrm{ch}}\xi\right), \quad \zeta = \frac{y}{H},\ \xi = \frac{h}{H}.$$

The integral in (3.59) is expressed in terms of a probability integral

$$\mathrm{Erfi}(z) = \frac{2}{\pi}\int_0^z e^{t^2}\mathrm{d}t,$$

and finally, it can be derived that the relative thickening depends on the front position as

$$\begin{aligned}\frac{1}{H}\int_0^h \varepsilon_y^{+}(y)\mathrm{d}y &= a\sqrt{\frac{\pi}{2}}\left(Q\frac{\tau_{+}}{T_{\mathrm{D}}}\right)^{1/2}\exp\left(-\frac{(T_{\mathrm{D}}\xi + T_{\mathrm{ch}})^2}{2Q\tau_{+}T_{\mathrm{D}}}\right)(\mathrm{Erfi}(z_2) - \mathrm{Erfi}(z_1)) \\ &+ \left(\beta\vartheta^{\mathrm{tr}} - \frac{(3k_{+} + 2\mu_2)}{3k_{+} + 4\mu_2}\varepsilon_0\right)\xi,\end{aligned} \tag{3.60}$$

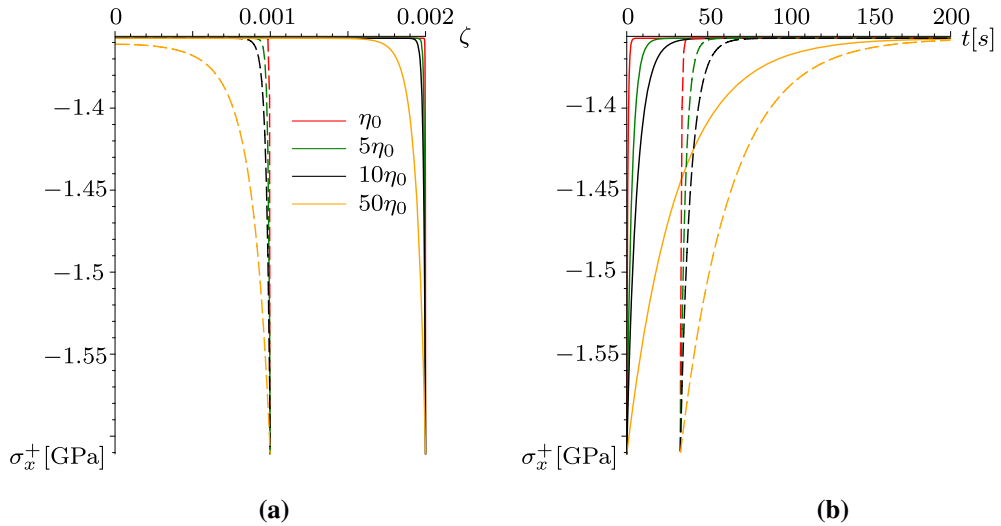

Fig. 13 Stress relaxation at various values of viscosity coefficient η for the standard linear solid model: **a** stress distributions behind the front for two front positions $\xi = 0.001$ (dashed lines) and $\xi = 0.002$ (solid lines), **b** stress relaxation in points $\zeta = 0.001$ (solid lines) and for $\zeta = 0.002$ (dashed lines); $\varepsilon_0 = 0$, $\eta_0 = 15.9$ GPa s. Solid and dashed lines of the same color correspond to the same viscosity coefficient

where

$$z_1 = \left(\frac{T_D}{2Q\tau_+}\right)^{1/2} \frac{T_{ch}}{T_D}, \quad z_2 = \left(\frac{T_D}{2Q\tau_+}\right)^{1/2} \left(\frac{T_{ch}}{T_D} + \xi\right) \tag{3.61}$$

The results of quantitative studies of stress relaxation and strains evolution and the redistribution of various modes of strains are shown in Figs. 13, 14, 15 and 16. Material parameters are given in Table 1. Two sets of the stress distributions behind the reaction front at two moments t_y which correspond to the front positions $\xi = 0.001$ and $\xi = 0.002$ and two sets of stress relaxation curves for stresses in points $\zeta = 0$ and $\zeta = 0.005$ are shown in Fig. 13 for various viscosity coefficients η. Note that the transformation strain may produce huge stresses at the reaction front which would remain in a pure elastic statement and might cause plastic strains and fracture. But one can see how narrow the high stresses domain can be and how fast the stresses may relax due to the viscous behavior of the reaction product at proper viscosities. This demonstrates that, in dependence of the viscosity, the stress relaxation can or cannot prevent damage accumulation and fracture at the reaction front.

Figure 14a, c demonstrates the time evolution of viscous strains in two points, illustrating how fast the limit values can be reached in dependence of the viscosity. Redistribution of the elastic and viscous strains within the total strain in point $\xi = 0$ is shown in Fig. 14b, d.

Figure 15 shows how the stress dependencies are affected by external strain. It is seen how the limit values of residual elastic stress are reached.

Relaxation times τ_+ and τ_1 do not depend on the energy parameter γ. But γ affects the front velocity and, thus, the front kinetics. Increasing γ increases the front velocity. The stress behind the front does not have enough time to relax, and the stress distribution becomes more smeared, as it is shown in Fig. 16a. If γ decreases, then the front propagates more slowly, and a sharper drop of the compressive stress σ_x takes place in the stress distributions behind the front.

The time dependencies of stress σ_x in points $\zeta = 0$ and $\zeta = 0.005$ for various γ are presented in Fig. 16b. Stress relaxation in point $\zeta = 0$ does not depend on γ, and the time dependence of the stress is presented by the solid black line. If $\zeta \neq 0$, then the stress relaxation starts at the moment t_y for $y = \zeta H$. By (3.28) and (3.29), if γ grows, then the parameter Q increases and, thus, the time t_y decreases, i.e., the relaxation starts earlier. One can see how the curves shift to the left when the gamma is increased. Note that the energy parameter depends on temperature, and the temperature may also affect stress relaxation via the viscosity coefficient.

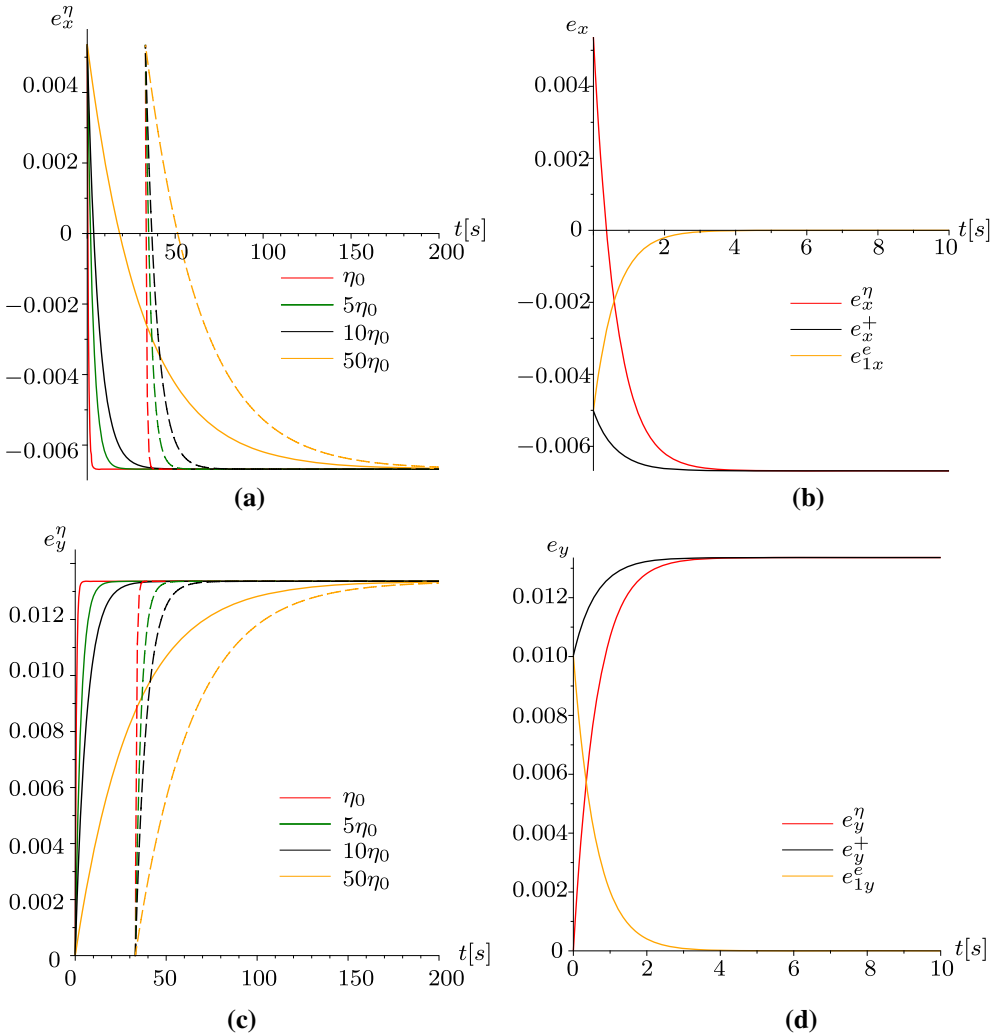

Fig. 14 Evolution and redistribution of viscous and elastic strains: **a**, **c** evolution of viscous strains e_x^η and e_y^η, respectively, in the point $\zeta = 0$ from the moment $t = 0$ and in the point y front the moment $t_y = 30\,\mathrm{s}$ for various viscosity coefficients; **b**, **d** redistribution of elastic strains e_{1x}^e, e_{1y}^e and viscous strains e_x^η, e_y^η within total strains e_x^+, e_y^+ in the point $\zeta = 0$. Solid and dashed lines of the same color correspond to the same viscosity

3.4 Particular cases of viscoelastic behaviors

In this subsection, we specify the equations for stresses and strains behind propagating reaction front for three rheological models which can be considered as particular cases of standard linear solid model and discuss the applicability of these models in the statement of mechanochemistry problems.

3.4.1 Maxwell material

We obtain the Maxwell material, as shown in Fig. 3b, from SLSM setting $\mu_2 = 0$, $\beta = 1$ and $\mu_1 = \mu_+$. The formula (3.24) for χ_0 remains the same with new μ_+. The formulae (3.40), (3.45), (3.48), (3.49) (3.50) for strains ϑ^+, e_x^+, e_{1x}^e and stresses σ_x^+ and σ_z^+ behind the front become

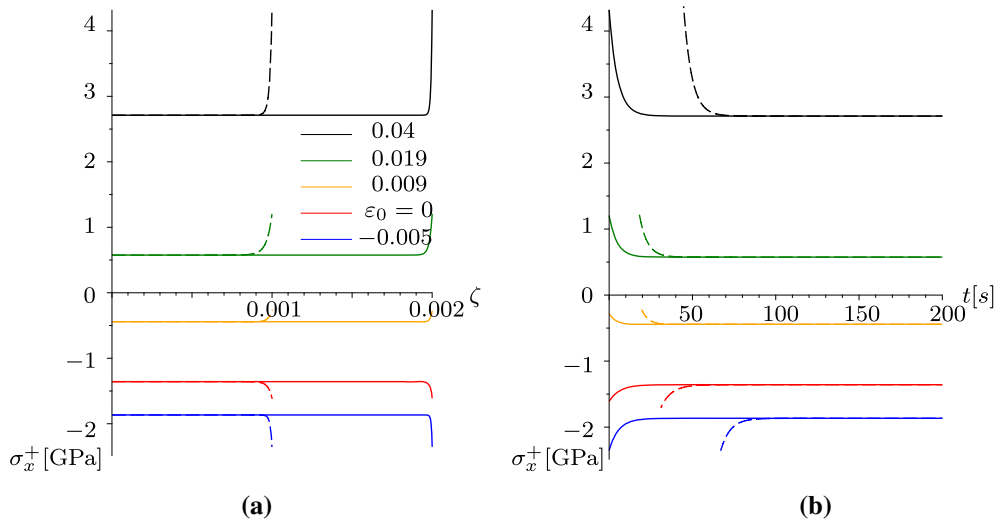

Fig. 15 Stress relaxation at various values of external strain ε_0: **a** stresses behind the front for two front positions $\xi = 0.001$ (dashed lines) and $\xi = 0.002$ (solid lines); **b** stress relaxation in two points $\zeta = 0.001$ and $\zeta = 0.002$. Solid and dashed lines of the same color correspond to the same external strains

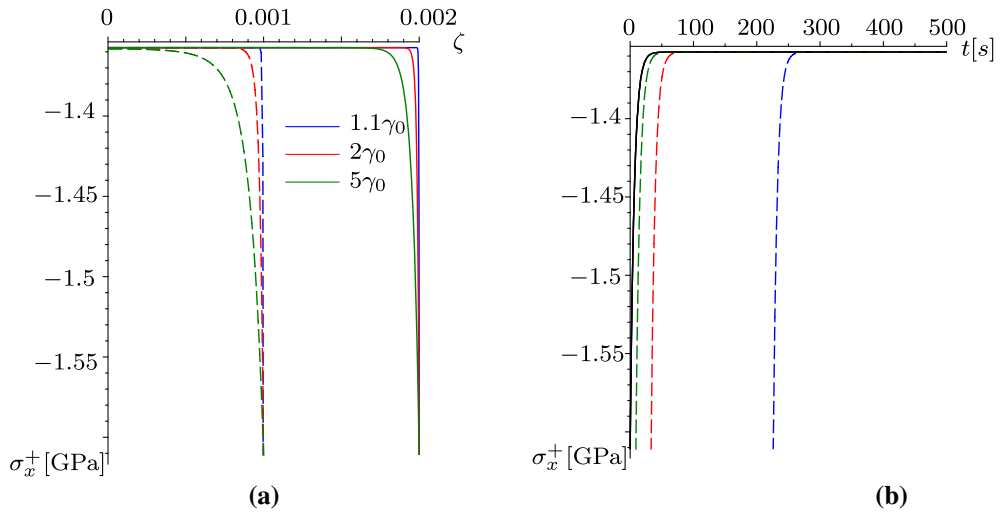

Fig. 16 Stress relaxation at various values of energy parameter γ for the standard linear solid model (solid and dashed lines of the same color correspond to the same energy parameter): **a** stresses behind the reaction front for two front positions $\xi = 0.001$ and $\xi = 0.002$; **b** stress relaxation in two points $\zeta = 0$ (the solid line) and $\zeta = 0.005$ (dashed lines)

$$\vartheta^+(y,t) = \vartheta^{\mathrm{tr}} + \frac{2\mu_+\left(3\varepsilon_0 - 2\vartheta^{\mathrm{tr}}\right)}{3k_+ + 4\mu_+}\exp\left(-\frac{t-t_y}{\tau_+}\right), \tag{3.62}$$

$$e_x^+(y,t) = \varepsilon_0 - \frac{\vartheta^{\mathrm{tr}}}{3} - \frac{2\mu_+\left(3\varepsilon_0 - 2\vartheta^{\mathrm{tr}}\right)}{3\left(3k_+ + 4\mu_+\right)}\exp\left(-\frac{t-t_y}{\tau_+}\right), \tag{3.63}$$

$$e_x^e(y,t) = \frac{k_+(3\varepsilon_0 - 2\vartheta^{\mathrm{tr}})}{2(3k_+ + 4\mu_+)}\exp\left(-\frac{t-t_y}{\tau_+}\right) + \frac{\varepsilon_0}{2}\exp\left(-\frac{t-t_y}{\tau_1}\right), \tag{3.64}$$

and

$$\sigma_x^+(y,t) = \frac{3k_+\mu_+\left(3\varepsilon_0 - 2\vartheta^{\mathrm{tr}}\right)}{3k_+ + 4\mu_+}\exp\left(-\frac{t-t_y}{\tau_+}\right) + \mu_+\varepsilon_0\exp\left(-\frac{t-t_y}{\tau_1}\right), \tag{3.65}$$

$$\sigma_z^+(y,t) = \frac{3k_+\mu_+\left(3\varepsilon_0 - 2\vartheta^{\mathrm{tr}}\right)}{3k_+ + 4\mu_+}\exp\left(-\frac{t-t_y}{\tau_+}\right) - \mu_+\varepsilon_0\exp\left(-\frac{t-t_y}{\tau_1}\right), \tag{3.66}$$

where

$$\tau_1 = \frac{\eta}{\mu_+}, \quad \tau_+ = \frac{(3k_+ + 4\mu_+)}{3k_+}\frac{\eta}{\mu_+}.$$

If $t \to \infty$, then $\vartheta^+(y,t) \to \vartheta^{\rm tr}$, $\varepsilon_y^+ \to \vartheta^{\rm tr} - \varepsilon_0$ and $\sigma_x^+ \to 0$, i.e., stresses totally relax. Since the conversion coefficient $\beta = 1$, the volume expansion resulting from the reaction is converted totally into the strain ε_y^+ at $\varepsilon_0 = 0$ (cf. with (3.57), (3.58) at $\mu_2 = 0$).

3.4.2 Kelvin–Voigt material

Another particular case is the Kelvin–Voigt material (Fig. 3c). In this case,

$$\mu_1 \to \infty, \ \mu_2 \to \mu_+, \tag{3.67}$$

$$\mathbf{e}^+ = \mathbf{e}^\eta = \mathbf{e}^e, \quad \boldsymbol{\sigma}^+ = k_+\left(\vartheta^+ - \vartheta^{\rm tr}\right)\mathbf{I} + 2\mu_+\mathbf{e}^+ + 2\eta\dot{\mathbf{e}}^+. \tag{3.68}$$

Since the dash-pot element cannot deform simultaneously, at the reaction front $\mathbf{e}^\eta = \mathbf{e}^+ = 0$. Then, this degenerative case can be realized only if $\varepsilon_0 = 0$. Then, $w_- = 0$ and at the reaction front

$$\vartheta = \vartheta(y, t_y) = 0. \tag{3.69}$$

Then, $\chi = w_+ = \frac{1}{2}k_+(\vartheta^+)^2$. Mechanics just subtracts $\frac{1}{2}k_+(\vartheta^+)^2$ from γ in the expression of $A_{\rm NN}$. Of course, this also directly follows from (3.24) and (3.25) if one takes the parameters according to (3.67).

The equation (3.38) for ϑ behind the front takes the form

$$\dot{\vartheta}^+ + \frac{\vartheta^+}{\tau} - \frac{3k_+}{4\eta}\vartheta^{\rm tr} = 0, \quad \tau = \frac{4\eta}{3k_+ + 4\mu_+}. \tag{3.70}$$

The solution, satisfying the initial condition (3.69), is

$$\vartheta^+(y,t) = \frac{3k_+\vartheta^{\rm tr}}{3k_+ + 4\mu_+}\left(1 - \exp\left(-\frac{t - t_y}{\tau}\right)\right). \tag{3.71}$$

The volume strain in points behind the front increases with time if $\vartheta^{\rm tr} > 0$. Since $e_x^+ = e_z^+ = -\vartheta/3$, from (3.68) and (3.71) it follows that the stresses behind the front can be expressed via ϑ and relax as

$$\begin{aligned}\sigma_x^+(y,t) = \sigma_z^+(y,t) &= -\frac{2}{3}\eta\dot{\vartheta}^+ + \left(k^+ - \frac{2}{3}\mu_+\right)\vartheta^+ - k_+\vartheta^{\rm tr} \\ &= -\frac{6k_+\mu_+\vartheta^{\rm tr}}{3k_+ + 4\mu_+}\left(1 + \frac{3k_+}{4\mu_+}\exp\left(-\frac{t - t_y}{\tau}\right)\right).\end{aligned} \tag{3.72}$$

At the reaction front

$$\sigma_x^+ = \sigma_z^+ = -\frac{3}{2}k_+\vartheta^{\rm tr}. \tag{3.73}$$

Of course, Eqs. (3.71), (3.73) and (3.73) directly follow from (3.40), (3.49) and (3.51) if to take μ_1 and μ_2 from (3.67), but, since this case may be of a special interest, we presented the short derivations (3.68)–(3.72).

3.4.3 Pure linear-viscous material

The linear-viscous material (Fig. 3d) can be obtained by setting $\mu_+ = 0$ in above formulae. It can be considered only at the same restriction $\varepsilon_0 = 0$ as above. Then, at the reaction front $w_- = 0$, $\chi = w_+ = \frac{1}{2}k_+(\vartheta^+)^2$,

$$\vartheta^+ = 0, \quad \sigma_x^+ = \sigma_z^+ = -\frac{3}{2}k_+\vartheta^{\mathrm{tr}}$$

It is easy to see that the volume strain in points behind the front increases up to $\vartheta^{\mathrm{tr}} > 0$ (decreases if $\vartheta^{\mathrm{tr}} < 0$) with time as

$$\vartheta^+(y,t) = \vartheta^{\mathrm{tr}}\left(1 - \exp\left(-\frac{t - t_y}{\tau}\right)\right), \quad \tau = \frac{4\eta}{3k_+} \tag{3.74}$$

and stresses relax as

$$\sigma_x^+(y,t) = \sigma_z^+(y,t) = -\frac{3}{2}k_+\vartheta^{\mathrm{tr}}\exp\left(-\frac{t - t_y}{\tau}\right) \tag{3.75}$$

Note that the restriction $\varepsilon_0 = 0$ makes the Kelvin–Voigt and pure viscous materials rather unsuitable than suitable as rheological models, as opposed the standard linear solid model and the Maxwell material. This indicates that not every common rheological model can be used for reaction constituents in the considerations of coupled problems of mechanochemistry.

4 Conclusions

The stress-affected chemical reaction front propagation in deformable solid in the case of a planar reaction front has been considered basing on the concept of the chemical affinity tensor. The influence of strains and material parameters on the kinetics of the front propagation was studied in detail with the use of the notion of the equilibrium concentration. Two types of the dependencies of the equilibrium concentration and, thus, front velocity on strain are demonstrated, depending on the relations between the combinations of elastic moduli of solid reactants. In the first case, the front can propagate only if strains belong to some interval, and it cannot propagate at all if the energy parameter is less than the critical value defined by the elastic moduli and transformation strain. In the second case, the front can propagate at any energy parameter at proper strains which are outside of a corresponding interval.

Different cases also correspond to different characters of the influence of strains on the acceleration or retardation of the reaction front. In the first case, increasing strains within the interval of allowed strains over the critical strain leads to reaction retardation. In the second case, increase of the absolute value of the strain out of the interval of forbidden strains accelerates the reaction front.

The changing of the rheological behavior of a solid constituent, sourced by a localized chemical reaction, was taken into account with the use of the standard linear solid model and its particular cases. The SLSM and Maxwell model allowed to obtain analytical solutions which gave us possibilities to study the specific effects of material parameters on stress relaxation behind the reaction front. On the other hand, the Kelvin–Voigt and pure viscous materials can hardly be considered as proper candidates for modeling the reaction products.

Results show that viscous deformations of the reaction product do not affect directly the kinetics of the front in the case of the SLSM if the external strain is applied along the interface plane, since they do not have time to appear at the moment of the transformation. But they enable the possibility for a stress relaxation phenomenon behind the reaction front and the accommodation of the transformation volume strain. Depending on the viscous and elastic parameters, this relaxation can be fast, and the high stresses region may be localized in a narrow layer adjacent to the transformation front. Note also that other external loadings are possible, at which stress relaxation can restart the initially blocked reaction front. Following these results, different perspectives could be drawn for coupled mechanochemistry simulations based on the chemical affinity tensor in order to be applied for more complex external loading and various geometries.

Acknowledgements ABF greatly appreciates the financial support provided by the Russian Science Foundation (Grant No. 19-19-00552). SP and ECh are grateful for the financial support provided by the Chaire André Citroën between Stellantis and Ecole Polytechnique

References

1. Brassart, L., Suo, Z.: Reactive flow in solids. J. Mech. Phys. Solids **61**(1), 61–77 (2013)
2. Buttner, C., Zacharias, M.: Retarded oxidation of Si nanowires. Appl. Phys. Lett. **89**, 263106 (2006)
3. Courtney, T.: Mechanical Behavior of Materials. McGraw-Hill, New York (2000)
4. Cui, Z., Gao, F., Qu, J.: Interface-reaction controlled diffusion in binary solids with applications to lithium ion batteries. J. Mech. Phys. Solids **61**(2), 293–310 (2013)
5. De Donder, T., Van Rysselberghe, P.: Thermodynamic Theory of Affinity: A Book of Principles. Stanford University Press, Stanford University, Stanford (1936)
6. Deal, E., Grove, A.: General relationship for the thermal oxidation of silicon. Appl. Phys. **36**, 3770–3778 (1965)
7. EerNisse, E.: Stress in thermal SiO_2 during growth. Appl. Phys. Lett. **35**, 8 (1979)
8. Freidin, A.B.: On chemical reaction fronts in nonlinear elastic solids. In: Indeitsev, D., Krivtsov, A.M. (eds.) Proceedings of the XXXVII Summer School–Conference Advanced Problems in Mechanics (APM 2009), St. Petersburg (Repino), June 30–July 5, 2009, pp. 231–237. Institute for Problems in Mechanical Engineering of Russian Academy of Sciences (2009)
9. Freidin, A.B.: Chemical affinity tensor and stress-assist chemical reactions front propagation in solids. In: Proceedings of the ASME 2013 International Mechanical Engineering Congress and Exposition, vol. 9, p. V009T10A102. American Society of Mechanical Engineers (2013)
10. Freidin, A.B.: On a chemical affinity tensor for chemical reactions in deformable solids. Mech. Solids **50**(3), 260–285 (2015)
11. Freidin, A.B., Korolev, I.K., Aleshchenko, S.P., Vilchevskaya, E.N.: Chemical affinity tensor and chemical reaction front propagation: theory and FE-simulations. Int. J. Fract. **202**(2), 245–259 (2016)
12. Freidin, A.B., Morozov, N.F., Petrenko, S.E., Vilchevskaya, E.N.: Chemical reactions in spherically-symmetric problems of mechanochemistry. Acta Mech. **227**(1), 43–56 (2016)
13. Freidin, A.B., Sharipova, L.L.: Forbidden strains and stresses in mechanochemistry of chemical reaction fronts. In: Altenbach, H., Pouget, J., Rousseau, M., Collet, B., Michelitsch, T. (eds.) Generalized Models and Non-classical Approaches in Complex Materials 1. Advanced Structured Materials, vol. 89, pp. 335–348. Springer, Cham (2018)
14. Freidin, A.B., Vilchevskaya, E.N.: Chemical affinity tensor in coupled problems of mechanochemistry. In: Altenbach, H., Öchsner, A. (eds.) Encyclopedia of Continuum Mechanics. Springer, Berlin (2020)
15. Freidin, A.B., Vilchevskaya, E.N., Korolev, I.K.: Stress-assist chemical reactions front propagation in deformable solids. Int. J. Eng. Sci. **83**, 57–75 (2014)
16. Gibbs, J.: The Collected Works of J.W. Gibbs, Volume 1: Thermodynamics. Yale University Press, London (1948)
17. Glansdorff, P., Prigogine, I.: Thermodynamic Theory of Structure, Stability and Fluctuations. Wiley, New York (1971)
18. Grinfeld, M.: Thermodynamic Methods in the Theory of Heterogeneous Systems. Longman, Sussex (1991)
19. Gurtin, M.: Configurational Forces as Basic Concepts of Continuum Physics. Springer, Berlin (2000)
20. Huang, C.K., Jaccodine, R.J., Butler, S.R.: Stress effect on the oxidation of silicon. In: Kapoor, V.J., Hankins, K.T. (eds.) Silicon Nitride and Silicon Dioxide Thin Insulating Film, vol. 87–10, pp. 343–349. The Electrochemical Society, Pennington (1987)
21. Jia, Z., Li, T.: Stress-modulated driving force for lithiation reaction in hollow nano-anodes. J. Power Sources **275**, 866–876 (2015)
22. Kao, D., McVitie, J., Nix, W., Saraswat, K.: Two dimensional thermal oxidation of silicon-II. Modeling stress effect in wet oxides. IEEE Trans. Electron Dev. **35**, 25–37 (1988)
23. Kienzler, R., Herrmann, G.: Mechanics in Material Space with Application to Defect and Fracture Mechanics. Springer, Berlin (2000)
24. Knowles, J.: On the dissipation associated with equilibrium shocks in finite elasticity. J. Elast. **9**, 131–158 (1979)
25. Knyazeva, A.: Cross effects in solid media with diffusion. J. Appl. Mech. Tech. Phys. **44**, 373–384 (2003)
26. Knyazeva, A.: Application of irreversible thermodynamics to diffusion in solids with internal surfaces. J. Non-Equilib. Thermodyn. **45**(4), 401–418 (2020)
27. Kobeda, E., Irene, E.: In situ stress measurements during thermal oxidation of silicon. J. Vac. Sci. Technol. B **7**, 163 (1989)
28. Krzeminski, C., Han, X.L.: Understanding of the retarded oxidation effects in silicon nanostructures. Appl. Phys. Lett. **100**, 26 (2012)
29. Levitas, V., Attariani, H.: Anisotropic compositional expansion and chemical potential for amorphous lithiated silicon under stress tensor. Sci. Rep. **3**, 1615 (2013)
30. Loeffel, K., Anand, L.: A chemo-thermo-mechanically coupled theory for elastic-viscoplastic deformation, diffusion, and volumetric swelling due to a chemical reaction. Int. J. Plasticity **27**, 1409–1431 (2011)
31. Maugin, G.: Configurational Forces: Thermomechanics, Physics, Mathematics, and Numerics. Chapman & Hall/CRC Press, Boca Raton (2011)
32. McDowell, M., Lee, S., Nix, W., Cui, Y.: 25th anniversary article: understanding the lithiation of silicon and other alloying anodes for lithium-ion batteries. Adv. Mater. **25**(36), 4966–4984 (2013)
33. Mihalyi, A., Jaccodine, R.J., Delph, T.J.: Stress effects in the oxidation of planar silicon substrates. Appl. Phys. Lett. **74**(14), 1981–1983 (1999)
34. Morozov, A.V., Freidin, A.B., Klinkov, V.A., et al.: Experimental and theoretical studies of Cu–Sn intermetallic phase growth during high-temperature storage of eutectic snag interconnects. J. Electron. Mater. **49**(12), 7194–7210 (2020)
35. Morozov, A.V., Freidin, A.B., Müller, W.H.: Stability of chemical reaction fronts in the vicinity of a blocking state. PNRPU Mech. Bull. **2019**(3), 58–64 (2019)
36. Muhlstein, C.L., Ritchie, R.O.: High-cycle fatigue of micron-scale polycrystalline silicon films: fracture mechanics analyses of the role of the silica/silicon interface. Int. J. Fract. **119**(120), 449–4745 (2003)
37. Nanko, M.: High-temperature oxidation of ceramic matrix composites dispersed with metallic particles. Sci. Technol. Adv. Mater. **6**, 129–134 (2005)
38. Palmov, V.: Vibrations of Elasto-Plastic Bodies. Springer, Berlin (1998)

39. Poluektov, M., Freidin, A.B., Figiel, L.: Modelling stress-affected chemical reactions in non-linear viscoelastic solids with application to lithiation reaction in spherical Si particles. Int. J. Eng. Sci. **128**, 44–62 (2018)
40. Poluektov, M., Freidin, A.B., Figiel, L.: Micromechanical modelling of mechanochemical processes in heterogeneous materials. Model. Simul. Mater. Sci. Eng. **27**, 084005 (2019)
41. Prigogine, I., Defay, R.: Chemical Thermodynamics. Longmans, Green, London (1954)
42. Reiner, M.: Rheology. Springer, Gottingen (1958)
43. Sutardja, P., Oldham, W.G.: Modeling of stress effects in silicon oxidation. IEEE Trans. Electron Dev. **36**(11), 2415–2421 (1988)
44. Vilchevskaya, E.N., Freidin, A.B.: On kinetics of chemical reaction fronts in elastic solids. In: Altenbach, H., Morozov, N. (eds.) Surface Effects in Solid Mechanics, pp. 105–117. Springer, Berlin (2013)
45. Wilmanski, K.: Thermomechanics of Continua. Springer, Berlin (1998)
46. Yen, J.Y., Hwu, J.G.: Enhancement of silicon oxidation rate due to tensile mechanical stress. Appl. Phys. Lett. **76**, 1834–1835 (2000)
47. Zhao, K., Pharr, M., Wan, Q., Wang, W., Kaxiras, E., Vlassak, J., Suo, Z.: Concurrent reaction and plasticity during initial lithiation of crystalline silicon in lithium-ion batteries. J. Electrochem. Soc. **159**, A238–A243 (2012)